Master's Thesis

Verifying the presence of voltage gated sodium channels in retinal pigment epithelium

Elina Hurskainen

University of Jyväskylä

Department of Biological and Environmental Science

Cell and Molecular Biology

29.11.2020

JYVÄSKYLÄN YLIOPISTO, Matemaattis-luonnontieteellinen tiedekunta
Bio- ja ympäristötieteiden laitos
Solu- ja molekyylibiologia

Elina Hurskainen	Jänniteherkkien natriumkanavien todentaminen verkkokalvon pigmenttiepiteelistä
Pro gradu -tutkielma:	58 s., 6 liitettä (22 s.)
Työn ohjaajat:	Soile Nymark, TkT, dosentti, Akatemiatutkija Julia Fadjukov, FM,
Tarkastajat:	Jari Ylänne, Ft, professori Teijo Kuopio, LKT, tutkimusjohtaja
Marraskuu 2020	

Hakusanat: ionikanava, kalvoproteiini, Na_V, proteiinineristys, RPE, silmä

Verkkokalvon pigmenttiepiteeli (eng. *retinal pigment epithelium* eli *RPE*) on välttämätön kudos näkökyvylle. RPE toimii esteenä verenkierron ja verkkokalvon välillä, huoltaa valoreseptorisoluja mm. kuljettamalla ravinteita ja absorboimalla haitallista, siroavaa valoa, sekä avustaa näköaistimuksessa. RPE:n toiminnan heikentyminen saattaa johtaa verkkokalvon rappeumaan sekä lopulta näkökyvyn menettämiseen. Ionikanavien rooli on merkittävä verkkokalvon pigmenttiepiteelin normaalille toiminalle. Tässä työssä tutkittiin RPE:n jänniteherkkiä natriumkanavia (*eng. voltage gated sodium channels* eli *Na_V);* tavoitteena oli vahvistaa erilaisten jänniteherkkien natriumkanavien alayksiköiden esiintyminen verkkokalvon pigmenttiepiteelissä kuvantamisen keinoin sekä eristämällä niitä RPE-soluista ja todentaa ne Western blot -menetelmällä. Aluksi kaikki yhdeksän Na_V –alayksikköä värjättiin sopivilla vasta-aineilla ja kuvattiin konfokaalimikroskoopilla. Ne alayksiköt, jotka havaittiin mikroskoopilla, oli määrä eristää RPE-soluista ja edelleen tutkia Western blot –menetelmän avulla. Ainoastaan $Na_V1.4$, $Na_V1.5$, $Na_V1.6$ ja $Na_V1.8$ voitiin luotettavasti havaita vasta-aineleimatuista solunäytteistä mikroskoopilla. Nämä em. jänniteherkän natriumkanavan alayksiköt valittiin siis jatkokäsittelyihin. Ennen varsinaista eristämistä ja Na_V-alayksiköiden olemassaolon vahvistamista, sopivin kalvoproteiinien eristysmenetelmä sekä tähän tarkoitukseen soveltuva Western blot –protokolla oli testattava ja optimoitava. Na_V-proteiinien

eristyksessä paras saanto saatiin radioimmunosaostuksen määrityspuskuri (*RIPA*), proteaasi-inhibiittoreiden ja etyleenidiamiinitetraetikkahapon (*EDTA*) yhdistelmällä. Eristetyt kalvoproteiinit eroteltiin toisista proteiineista SDS-geelielektroforeesin avulla, siirrettiin sähkövirran avulla nitroselluloosakalvolle ja lopuksi värjättiin sopivilla vasta-aineilla. Tutkimuksissa varmistui edelleen, että RPE solut selvästi ilmentävät $Na_V1.4$, $Na_V1.5$ ja $Na_V1.6$ alayksiköitä. Tulokset viittasivat vahvasti siihen, että RPE ilmentäisi myös alayksikköä 1.8, mutta tämän kohdalla Western blot –tulokset eivät olleet yhtä selkeitä kuin muilla alayksiköillä. $Na_V1.8$ luotettava todentaminen vaatii siis vielä työtä ja mahdollisesti protokollien uudelleen optimointia.

UNIVERSITY OF JYVÄSKYLÄ, Faculty of Mathematics and Science
Department of Biological and Environmental Science
Cell and Molecular Biology

Elina Hurskainen	Verifying the existence of voltage gated sodium channel in retinal pigment epithelium
MSc thesis:	58 pages, 6 Appendices (22 pages)
Supervisors:	Soile Nymark, D.Sc. (Tech.), Docent Julia Fadjukov, FM
Inspectors:	Jari Ylänne, PhD, professor Teijo Kuopio, D.Med.Sc., research director

November 2020

Keywords: eye, ion channels, membrane proteins, membrane protein extraction, retina

The retinal pigment epithelium (*RPE*) is an important tissue for vision. It functions as a barrier between retina and blood circulation but also takes care of the light sensing cells of the retina cells and aids with vision. The loss of different functions in RPE has been linked with retinal dysfunction and degeneration which can finally lead to the loss of vision. Ion channels have been discovered to be very important for the normal function of RPE and for visual health. The aim of this study was to verify the presence of different voltage gated sodium channel subunits (Na_V) in RPE. All nine Na_V subunits ($Na_V1.1$-1.9) were assayed with suitable fluorescent antibodies from RPE cells and the results were examined with confocal microscopy. Only four Na_V subunits, $Na_V1.4$, $Na_V1.5$, $Na_V1.6$ and $Na_V1.8$, were visibly abundant in the RPE cells. These Na_V subunits needed to be extracted and immunoblotted. Before the verifications, the protocols for membrane protein extraction and immunoblotting were developed and optimised. The best extraction results were obtained with a combination of radioimmunoprecipitation assay buffer (*RIPA*), protease inhibitor cocktail and ethylenediaminetetraacetic acid (*EDTA*). The extracted sodium channel subunits were separated from other proteins with SDS gel electrophoresis, transferred into a nitrocellulose membrane and finally stained

with suitable antibodies. Taken together, the results verified the presence of $Na_V1.4$, $Na_V1.5$ and $Na_V1.6$ subunits in RPE cells. The $Na_V1.8$ was only slightly visible in the blots, so the existence could not be confirmed. However, all the results indicate that the RPE also expresses the $Na_V1.8$ subunit, but this still requires some additional work.

TABLE OF CONTENTS

TABLE OF CONTENTS 6
ABBREVIATIONS 8
1 INTRODUCTION 10
1.1 Retinal Pigment Epithelium – Crucial building block for vision 10
1.2. Ion channels are essential for RPE functions 12
1.2.1 Voltage gated sodium channels 14
1.3. Membrane protein extraction – not an easy task 15
1.4. Aim and goals of the study 19
2 MATERIALS AND METHODS 20
2.1 Cell lines and cell culture 20
2.2 Immunofluorescent staining of the Na_V subunits 21
2.3 Imaging immunoassayed cells and analysing the images 22
2.4 Membrane protein extraction 23
2.5 Optimising Western blot method 24
2.6 Molecular Weight analysis of the blots 26
3 RESULTS 28
3.1 Immunoassay and LSCM imaging 28
3.2 Na_V extraction and Western blot 32
4 DISCUSSION 39
ACKNOWLEDGEMENTS 52
REFERENCES 53
Appendices 59
Appendix 1: Reagents 59
Appendix 2: Immunofluorescence staining protocol 62

Appendix 3: Membrane protein extraction protocol 63

Appendix 4: Western blot protocol 65

Appendix 5: Original Western blot images 68

Appendix 6: Western blot MW determination 70

ABBREVIATIONS

BSA	Bovine serum albumin
EDTA	Ethylenediaminetetraacetic acid
ECL	Enhanced chemiluminescence
hESC	Human embryonic stem cell
hESC-RPE	Human embryonic stem cell derived retinal pigment epithelium cell
iPSC	Induced pluripotent stem cell
iPSC-RPE	Induced pluripotent stem cell derived retinal pigment epithelium cell
MW	Molecular weight
Na_V	Voltage gated sodium channel
PBS	Phosphate buffered saline
RIPA	Radioimmunoprecipitation assay buffer
RPE	Retinal pigment epithelium
RT	Room temperature
SB	Sample buffer
SDS-PAGE	Sodium dodecyl sulphate polyacrylamide gel electrophoresis
WB	Western blot method

1 INTRODUCTION

1.1 Retinal Pigment Epithelium – Crucial building block for vision

The retinal pigment epithelium (RPE) is a crucial element for coherent vision, and it has a very distinguishing phenotype: the hexagonal cells have dark, cytosolic melanin granules, and the cells form a tightly packed, pigmented monolayer (Strauss 2005, Wimmers et al. 2007). The RPE is located in the fundus of the eye between photoreceptors of the retina and choroid where it functions as a blood-retina barrier by separating photoreceptors from direct contact from the blood stream (Bok 1993, Kniesel and Wolburg 1993, Wimmers et al. 2007).

The RPE layer has the polar structure typical of all epithelia, that enables multiple special and significant functions (Strunnikova et al. 2010). The apical side of the plasma membrane faces the photoreceptors whereas the basolateral side is in touch with the multi-layered Bruch's membrane (Fox and Steinberg 1992, Strunnikova et al. 2010). The Bruch's membrane separates the basolateral side of the RPE from the capillaries (Wimmers et al. 2007). As a part of the blood-retina barrier, the basolateral side and Bruch's membrane are also the contact area where nutrients (e.g. glucose, fatty acids, vitamin A), water, metabolic products, ions and signalling molecules are exchanged between blood stream and the RPE (Bok 1993, Fox and Steinberg 1992, Wimmers et al. 2007). On the apical side long microvilli of the RPE surround the outer segments of the photoreceptors and enable close interaction of the two tissues (Fox and Steinberg 1992, Wimmers et al. 2007).

The RPE sustains photoreceptor homeostasis which is vital for maintaining visual health (Bok 1993, Kuznetsova et al. 2014, Strauss 2005). To maintain the retinal homeostasis the RPE secretes signalling molecules, immunosuppressive and growth factors to stabilise the structural integrity of the retina and to communicate with the surrounding cells and tissues (Strauss 2005). In addition, the RPE defends the adjacent tissues by extracting antioxidants, and the cytosolic pigmentation

absorbs damaging scattered light focused on the retina (Bok 1993, Strauss 2005, Wimmers et al. 2007). The RPE also has a role in visual cycle in the retina by regenerating 11-cis-retinal which functions as a chromophore in the photoreceptors in the phototransduction cascade (Bok 1993, Strauss 2005). The RPE takes care of the photoreceptors also by phagocyting shed photoreceptor outer segments (POS) from the subretinal space (Bok 1993, Moody and Robertson 1960, Young 1967).

Because the RPE is essential for vision dysfunction in functions of the tissue may result in death of visual cells, decay of the retina and even blindness (Jha and Bharti 2015, Kuznetsova et al. 2014, Sparrow et al. 2010, Strauss 2005). Degeneration of the RPE is linked e.g. to pathogenesis of age-related macular degeneration (ADM) which is a leading cause of blindness in western countries (Fine et al. 2000, Jager et al. 2008, Strauss 2005). There are multiple possibilities that might initiate retinal degeneration and loss of RPE functions such as disturbance with the visual cycle, an increase in oxidative stress, reduced capability to absorb the energy of the scattered light, accumulation toxic particles and chromophores and (Sparrow et al. 2010, Strauss 2005). Mutations and genetic vulnerability in RPE may also lead to retinal degeneration (Sparrow et al. 2010). The phagocytosis of the POS is also thought to eventually damage the RPE because POS particles accumulate in the aging RPE which in turn might compromise the normal function of the tissue (Bok 1993, Strauss 2005).

Under physiological circumstances, the RPE cells are not suspected to renew themselves by cell division after differentiation and damaged tissue is therefore not repaired (Bok 1993, Fronk and Vargis 2016). This further accelerates photoreceptor degeneration and loss of vision (Strauss 2005). There are undergoing studies aiming to produce an artificial RPE transplant to replace damaged RPE, rescue photoreceptor function and possibly even restore already lost vision (Fronk and Vargis 2016, Jha and Bharti 2015, Mazzoni et al. 2014). RPE cells are therefore an interesting target for gene therapy studies and the research for finding the most

efficient method to restore damaged RPE and vision are still ongoing (Jha and Bharti 2015, Sparrow et al. 2010).

1.2. Ion channels are essential for RPE functions

Ion channels have critical roles in physiology of all cells and RPE cells are no exception. Ion channels help to sustain the homeostasis of photoreceptors (Reichhart and Strauß 2014, Wimmers et al. 2007). Alterations in ion channel function or activity may lead to dysfunction of the RPE and degenerative diseases of the retina (Wimmers et al. 2007). Understanding how ion channels function in the RPE is essential for comprehending cell physiology and pathology of many retinal diseases (Reichhart and Strauß 2014, Wimmers et al. 2007).

Ion channels are specialized protein with an opening through a membrane via which ions can pass through to the other side of the membrane (Vinothkumar and Henderson 2010). Selective ion channels let only particular ions to pass through, whereas non-selective channels have wide pores through which ions travel according to an electrochemical or a concentration gradient (Vinothkumar and Henderson 2010). Ion channel opening can be regulated by voltage or a ligand (Vinothkumar and Henderson 2010).

The RPE expresses voltage-gated and ligand activated potassium, chloride and calcium ions (K^+, Cl^- and Ca^{2+} respectively) channels and they have a wide range of duties in retina (Reichhart and Strauß 2014, Wimmers et al. 2007). In the RPE these channels are involved for example in intracellular ion homeostasis, control cell cycles, trans-epithelial ion, water, nutrient and electrolyte transportation (Reichhart and Strauß 2014, Wimmers et al. 2007). Calcium, potassium and chlorine channels also regulate different steps of phagocytosis, photoreceptor dark adaption, pH, growth factor secretion intracellular and subretinal volume of the RPE (Reichhart and Strauß 2014, Wimmers et al. 2007). The focus of this study was, however, voltage gated sodium (Na_V) channels, and they are covered in more detail in the

next section.

Because the previous evidence has shown that Na_V channels are expressed in non-excitable cells and that RPE expresses other voltage gated ion channels, Na_V could also have significant purpose in the RPE. Indeed, there are physiological data and patch clamp measurements providing evidence that also RPE expresses the Na_V channels (Wimmers et al. 2007). However, until Johansson et al. (2019) proved the presence Na_V channels in the RPE there were no evident data about the actual function and significance of the Na_V channels in the RPE.

Na_V channels have traditionally been considered to be present only in excitable cells such as neurons and muscles (REF). According to Botchkin and Matthews (1994) the native RPE cells in the target organism might not actually be able to express Na_V channels and that their findings indicate that Na_V channel expression in RPE is a trait that emerges only in cultured cells (Botchkin and Matthews 1994).

Johansson et al., (2019), however, have discovered that Na_V channels are not just cultural trait in the RPE but are crucial for the function of the tissue. The absence of Na_V-mediated currents in freshly isolated RPE cells is most likely resulted from the destruction of tight junctions during enzymatic extraction: there is strong evidence there are functional Na_V channels present in RPE cells with intact cell-cell junctions (Johansson et al. 2019). In their experiments, Johansson and others (2019), also demonstrated that in RPE Na_V channels are clearly involved POS phagocytosis. The fact that RPE expresses such a versatile array of Na_V channels suggests that these channels might have other significant roles in RPE yet to be discovered (Johansson et al. 2019). Na_V channels could also be one of the key factors when studying the possible causes of the retinal degeneration and blindness – inhibition or weakening of the phagocytosis is predicted to be one of the possible causes for ADM, for example (Fronk and Vargis 2016, Jha and Bharti 2015, Mazzoni et al. 2014). Na_V channel presence was proved by Johansson et al. (2019) by Western blot, and the optimising process was studied in this project.

1.2.1 Voltage gated sodium channels

Sodium channels are crucial membrane proteins for cell homeostasis: Sodium ions (Na^+) carry out the charge in excitable cells, are involved in amino acid, sugar and neurotransmitter transport processes, pH and volume regulation of the subretinal space, removal of metabolic product (Wimmers et al. 2007). Dysfunction of the voltage-gated sodium (Na_V) channels has been associated with various neurological, cardiovascular and excitability disorders, including epilepsy, multiple sclerosis, peripheral neuropathy, neuropathic pain, muscle diseases and cardiac disorders (Black and Waxman 2013, Ahern et al. 2016, Yan et al. 2017).

Na_V channels are pore forming, Na^+ ion-conducting voltage sensors which are located on the intracellular, organelle-surrounding and plasma membrane (Black and Waxman 2013, Vinothkumar and Henderson 2010). The function of the Na_V channel is based on selective permeation of sodium ions in response to changes in the membrane voltage (Kwong and Carr 2015). There are three major phases with Na_V channel function: voltage-dependent activation, rapid inactivation and selective ion conductance (Yu and Catterall 2003). Na_v channels modulate between open and closed conformational states in the process of activation and inactivation and therefore enable or prevent the Na^+ flow (Kwong and Carr 2015, Marban et al. 1998).

In mammals, the family of Na_V channels consists of ten functionally related α subunits: $Na_V1.1$-$Na_V1.9$ and Na_x which are expressed in large variety of tissues (Marban et al. 1998, Loussouarn et al. 2016, Wood and Baker 2001). The subunits $Na_V1.1$-$Na_V1.9$ are encoded by different genes and they all have different functional roles but have identical topology and share more than 75% identical amino acid sequences (Wood and Baker 2001, Yan et al. 2017). Small differences between Na_V subunit genes contribute to the specialised and different functional roles (Yu and Catterall 2003).

Na_V channels are responsible of conducting muscle contraction, electrical impulses

and action potential in electrically excitable cells such as neurons, heart and muscles (Catterall 2000 Kwong and Carr 2015, Marban et al. 1998, Yan et al. 2017). Na_V channels are also targets of activity blocking actions of many drugs, natural toxins, animal and plant venoms (Ahern et al. 2016, Kwong and Carr 2015, Marban et al. 1998).

The Na_V channels are found almost solely in excitable cells and especially neurons express multiple Na_V subunits (Kwong and Carr 2015, Wimmers et al. 2007). $Na_V1.1$-1.3 and 1.6 are the primary subtypes in the brain, spinal cord and central nervous system, $Na_V1.4$ is abundant in the skeletal muscle, $Na_V1.5$ is usually expressed in the heart and cardiac muscle, and the subunits $Na_V1.7$-1.9 function mainly in the peripheral neurons (Black and Waxman 2013, Kwong and Carr 2015, Loussouarn et al. 2016, Wood and Baker 2001, Yan et al. 2017). There is now also convincing evidence from patch-clamp studies that various non-excitable cells can also express Na_V channels (Black and Waxman 2013). Every Na_V subunit has been discovered in some type of non-excitable cell which include for example astrocytes, NG2 cells, microglia, macrophages and some cancer cells (Black and Waxman 2013). In non-excitable cells Na_V channels have been discovered to contribute to phagocytosis, motility, release of biomolecules, regulation of Na^+/K^+-ATPase and metastasis activity (Black and Waxman 2013). Considering these findings and the fact that one of the most important functions of the RPE is POS phagocytosis, RPE cells should also express Na_V channels (Black and Waxman 2013).

1.3. Membrane protein extraction – not an easy task

Membrane protein characteristics have greatly limited their research by creating variety of challenges such as over-expressing them in other systems, solubilisation, purification, crystallisation, data collection and structure biology (Carpenter et al. 2008, Seddon et al. 2004, Wu and Yates 2003). Membrane embedded, i.e., integral membrane proteins are laborious and difficult to isolate and study due to their hydrophobicity, flexibility, low abundancy and instability, especially in aqueous

solutions and outside of their native membrane (Carpenter et al. 2008, Speers and Wu 2007, Vinothkumar and Henderson 2010). These are the biggest reasons, why membrane proteins are so underrepresented in protein databases (Santoni et al 2000).

Membrane proteins are classified into peripheral and integral membrane proteins based on the level of interaction with membrane. Integral membrane proteins interact strongly with the lipid bilayer by hydrophobic interactions (Santoni et al. 2000). Integral membrane protein span through the lipid bilayer multiple times (Santoni et al 2000, Speers and Wu 2007, Vinothkumar and Henderson 2010). The hydrophobic core of the membrane bilayer is the key factor for the structure of integral membrane proteins which enables their function (Speers and Wu 2007). Integral membrane proteins have hydrophobic and hydrophilic domain, in other words they are amphipathic (Wu and Yates 2003). The membrane spanning, i.e., the transmembrane regions are composed largely of the hydrophobic amino acid residues (Santoni et al 2000, Speers and Wu 2007). Na_V channels are also integral membrane proteins (REF).

The primary difficulty of membrane protein research is obtaining the protein of interest from the target membrane (Seddon et al. 2004). Membrane proteins should be extracted from sources in which the desired protein is naturally abundant (Von Jagow et al. 2003). Membrane proteins can be extracted from a variety of cells, tissues and organisms (Von Jagow et al. 2003). The source material can be broken down for example by using physical glass bead milling, ultra-sonification, osmotic shock, repeating freezing-thawing cycles or by using enzymatic lysis (Von Jagow et al. 2003).

Na_V channels are large (260 kDa) proteins with multiple membrane spanning regions (REF). Na_V channels consist of a core alpha (α) subunit and a supporting beta (β) subunit which controls the expression and activity of the pore forming segments (Kwong and Carr 2015, Loussouarn et al. 2016, Yan et al. 2017). The α

subunit forms the channel pore which is selectively permeable to Na^+ ions and determines conducting properties of the channel (Marban et al. 1998). Mammalian Na_V α subunits are composed of four domains each of which contribute to the selective ion filtration (Catterall 2000, Marban et al. 1998, Vinothkumar and Henderson 2010, Yu and Catterall 2003). The β subunit modulates the Na_V channel function, activation kinetics, inactivation, Na^+ currents and regulates the expression and membrane trafficking via the α subunit (Marban et al. 1998, Yan et al. 2017). These factors complicate the isolations of Na_V proteins from their native membranes.

Multiple protein extraction and purification steps result in a loss of target protein, so the process usually requires large quantities of material (Seddon et al. 2004, Wu and Yates 2003). However, compared to cytosolic and soluble proteins, the abundancy of membrane protein is low in their native membrane (Seddon et al. 2004, Wu and Yates 2003). Physiochemical properties of membrane proteins make them insoluble in water without detergents (Seddon et al. 2004, Speers and Wu 2007, Wu and Yates 2003). In addition, extracted membrane proteins isolated from their native membrane are often unstable and easily form aggregates in aqueous environment even with the presence of detergents (Carpenter et al. 2008, Matar-Merheb et al. 2011, Von Jagow et al. 2003).

Due to the weaker interactions with lipid bilayers the peripheral membrane proteins are easy to extract with milder techniques such as changes in pH, metal chelators, organic solvents or high saline buffers (Speers and Wu 2007, Ohlendieck 1996, Vinothkumar and Henderson 2010). Highly hydrophobic, membrane embedded integral proteins, however, require detergents to be solubilised and isolated (Carpenter et al. 2008, Ohlendieck 1996, Seddon et al. 2004, Von Jagow et al. 2003). Detergents mimic the natural membrane environment by forming micellar structures in aqueous environment and surround the hydrophobic surface of the membrane proteins and therefore enable integral membrane proteins to be solubilised without denaturation and aggregation (Matar-Merheb et al. 2011,

Ohlendieck 1996, Seddon et al. 2004, Speers and Wu 2007, Von Jagow et al. 2003). It is crucial to choose the right detergent to minimise aggregation and degeneration, to stabilise the protein structure, to purify the protein efficiently to produce the best yield (Carpenter et al. 2008, Damian et al. 2006, Von Jagow et al. 2003).

During the membrane protein isolation and purification processes there are usually large material losses in each step (Von Jagow et al. 2003). Optimising the protocols well and keeping isolation steps to a minimum prevents excess material and protein activity loss (Von Jagow et al. 2003). Optimising generally involves thorough testing of detergent types and concentration, possible pH effect, isolation steps, protease inhibitors and possible stabilising additives (Von Jagow et al. 2003). Poor lysis of the cells may lead to poor protein extraction. Therefore, the choice of the lysis buffer is important to ensure efficient protein solubility and stability (Gräslund et al. 2008, Von Jagow et al. 2003). The best lysis buffers contain a strong buffer (e.g. phosphate or HEPES), high ionic strength, protease inhibitors, a reducing agent (e.g. mercaptoethanol or dithiothreitol i.e. *DTT*) and additives such as EDTA (Gräslund et al. 2008). Other pitfalls during protein extraction that can lead to excess protein loss are insufficient removal of soluble proteins, the expression or purification of wrong recombinant proteins, contamination of additional proteins or multiple protein species, aggregation of the purified proteins, precipitation or failures in concentrating the sample for further studies. Furthermore, loss of protein material can occur if the equipment, lysates and the reagents are not cold enough (Gräslund et al. 2008, Ohlendieck 1996, Von Jagow et al. 2003).

After the protein extraction, the membrane proteins can be further studied and characterised by separating proteins of the lysate by gel electrophoresis followed by Western blot (Gräslund et al. 2008 Speers and Wu 2007, Wu and Yates 2003).

1.4. Aim and goals of the study

The aim of the study was to investigate if the RPE cells truly express Na_V channels and which of the subunits can be identified from this tissue. All of the nine subunits were stained with antibodies and results were examined with confocal microscopy. The subunits observed with microscopy were then supposed to be extracted and the existence of these subunits was confirmed with Western blot method. The project also included the optimisation of all methods needed.

2 MATERIALS AND METHODS

The study began by immunostaining all nine Na_V subunits from induced pluripotent stem cell derived RPE (iPSC-RPE) cells and imaging them with laser scanning confocal microscopy. The project continued with optimising a protocol for extracting integral membrane proteins and then analysing the lysate with a Western blot. The optimisations were carried out with ARPE-19 cells. ARPE-19 is a spontaneously arisen which is fast growing, easily expandable RPE cell line which expresses many RPE traits and functions (Dunn et al. 1996).

After the most suitable protocols were discovered and the necessary methods were optimised, the Na_V subunits observed with confocal microscopy were extracted from hESC-RPE. The isolated membrane proteins were immunoblotted to examine the success of the extraction and to verify the presence of the subunits. The detailed information of all the reagents used in this experiment is enlisted in APPENDIX 1.

2.1 Cell lines and cell culture

Immunoassays were executed with iPSC-RPE control cells (iPSC-RPE USA control, Cat#006-1-1, pl. 9/27/16, pl. 2/23/17, 120 000 cells/ml). These cells were maintained on Matrigel (Corning, Cat#734-0268) coated cell culture inserts (24-well Millicell® Hanging Cell Culture Insert, 1.0 μm PET, Cat# MCRp24H48) that were placed in a 24-well plate. The cells were cultured in a humidified incubator, kept at 37 °C in 5% CO_2. The growth medium (RPEM, Cat# SKU. No. A3359DJ, LAgen Laboratories) with 1 % fetal bovine serum (FBS, Cat# 10270-106, Gibco) and supplemented with 1 % Anti-Anti antibiotics solution (Cat# 15240-062, Gibco) was changed three times per week. The volume of the medium inside the cell culture insert was 300 μl and 700 μl under the insert. The differentiation of the iPSC-RPE was not included in this project.

The ARPE-19 were thawed and passaged in a T75 cell culture flask and maintained at +37°C in a humidified incubator (5 % CO_2) with growth media (DMEM/F-12 + GlutaMAX™, Cat# 31331-028, Gibco) containing 10 % FBS and supplemented with 1 % penicillin-streptomycin solution (Cat# DE17-602E, Lonza). The medium was changed twice a week. The ARPE-19 cells were routinely passaged every three to four weeks.

The hESC-RPE cells (08/017 sced p60, DM- + Bl. 07.10.16, pl. 11.01.17, freezed 23.02.2017) were differentiated, cultured and frozen prior to this project by Prof. Heli Skottman's research group (Tampere University). These cells were obtained from nitrogen gas phase and thawed prior to the lysis step.

2.2 Immunofluorescent staining of the Na_V subunits

The membranes of the cell culture inserts were removed and cut into four pieces with a scalpel. Each labelling was assayed in duplicates and the insert pieces were placed in a well plate where the immunostaining procedure was executed.

The samples i.e. the insert pieces were rinsed few times with 1x PBS (Cat# Lonza) and fixed with ice cold methanol (Cat# 32213-2.5L-M, Sigma) by incubating for 15 minutes in a hood at room temperature. Next, the samples were washed 3 x 5 min with PBS after which the cells were permeabilised with 0.1 % Triton™ X-100 (Cat# Sigma-Aldrich) in 1x PBS at room temperature for 15 minutes. After permeabilization, the possible unspecific binding of the antibodies and background were blocked with 3 % Bovine Serum Albumin (BSA, Cat# A8022-50G, Sigma® Life Science) in PBS for one hour at room temperature.

Next, the primary antibodies were prepared in blocking buffer (3 % BSA in PBS), added on the samples and incubated for one hour at room temperature with gentle agitation. Each of the nine Na_v subunit were examined from iPSC-RPE cells by staining them with Na_V channel subunit specific antibodies (Abcam and Alomone Labs) and by imaging them with laser scanning confocal microscopy (LSCM). A

tight junction protein marker zonula occludens 1 (ZO-1, Life Technologies) was chosen as a control stain to evaluate the success of the staining. Each of the different Na_V α subunit binding antibodies were prepared in different microcentrifuge tube with the presence of ZO-1. The more detailed information of the antibodies and the dilutions can be found in the APPENDIX 1.

After incubation, the primary antibodies were discarded, and the samples were washed 3 x 5 min with PBS. Next, the samples were stained with secondary antibodies (Alexa-Fluor 488 (ZO-1) and Alexa-Fluor 568 (Na_V subunit); Life Technologies) which were diluted in 3% BSA in PBS. Secondary antibodies were incubated for an hour in dark (RT). Finally, the samples were washed with PBS and mounted between two coverslips with ProLong Gold antifade reagent with DAPI (Cat# P36935, Molecular Probes). The more detailed immunostaining protocol can be found in the APPENDIX 2.

2.3 Imaging immunoassayed cells and analysing the images

The immunoassayed samples were imaged with Zeiss laser scanning confocal microscope 780 (LSCM, a, 780, AxioObserver) on inverted Zeiss Cell Observer microscope (Zeiss, Jena, Germany). Samples were imaged using Plan-Apochromat 63x/ 1.4 oil immersion objective (63x/1.40 Oil DIC M27). The Alexa Fluor 405 (DAPI) was excited with 405nm diode laser; Alexa Fluor 488 (anti-ZO-1 and anti-$Na_V1.2$) with 488 nm laser line from Argon laser; Alexa Fluor 568 (anti-Na_V) and TRITC with 561 nm DPSS or 562 nm InTune laser. Emission was detected with windows of (in nm) 410–495 (DAPI, Alexa Fluor 405), 499–579 (Alexa Fluor 488) and 579–642 (Alexa Fluor 568). Laser powers were kept to a minimum to avoid sample bleaching. From each sample, pixel stacks (Z-stack) of 100–140 slices (150 nm each) were acquired. The data was saved in .czi format.

The images stacks were analysed and processed with ImageJ software (Schneider et al. 2012). A maximum intensity projection (MIP) was taken from the 488 nm (ZO-1) and 568 nm (Na_V) channels of each image. DAPI channels were left out from these analyses because the signal was weak due to the cell pigmentation. The Na_V and ZO-1 channels were merged to examine the colocalization between Na_V channels and ZO-1 in the tight junctions. Finally, the MIP images were merged to create a montage of the different images.

2.4 Membrane protein extraction

Optimising process included testing lysis buffers and different, efficient methods to extract membrane proteins. After each test run some features were adjusted or, if the method did not produce any results, it was abandoned. Adjustable features were the number of cells used for extraction, the use and amount of protease inhibitors and the volume of the lysis buffer.

Membrane protein extraction was experimented with a few different methods before the discovery of the best yielding extraction method to be further optimised. First, a commercial extraction kit (ProteoExtract® Native Membrane, Cat# 444810, Calbiochem®) was tested. The extraction was executed with the instructions of the manufacturer from adherent cells in a cell culture flask and from a frozen cell pellet which was pelleted prior to this experiment. The second method to be tested was extracting the proteins directly into 2x Laemmli loading bufferobtained from Professor Vesa Hytönen's research group (Tampere University). Another membrane extraction protocol tested was using Triton X-114 solution. This method was done according to the instructions of Taguchi and Schätzl (2014). The protocol and instructions are based on the method used in research of Bordier 1981, and which of Taguchi and others had been modified (2013).

The final method tested was to use radioimmunoprecipitation assay buffer (RIPA) [50 mM Tris-HCl pH 7.4, 1 % NP-40, 0.5 % sodium deoxycholate, 0.1 % SDS, 150 mM NaCl, 100 mM Na-orthovanadate]. Extraction with RIPA was done according to the instructions of Abcam ("Sample preparation for Western blot") and the protocol was optimised for this purpose. First, the cell culture flask was placed on ice, growth medium was removed, and the cells were washed with cold PBS. Protease inhibitor cocktail (Cat# 87786, Thermo Scientific) and EDTA (Cat# 87786, Thermo Scientific) were added into the RIPA buffer and pipetted on cells. The adherent cells were removed from the bottom of the cull culture flask by scraping and then pipetted into a pre-cooled micro centrifuge tube. The cell lysate was incubated at +4 °C with gentle agitation for 30 minutes. After the incubation, the lysate was centrifuged at +4 °C, 12 000 rfc for 20 minutes. The supernatant containing the membrane proteins was collected and the pellet containing the cell organelles, soluble proteins and other debris was discarded. When executing this protocol with hESC-RPE cells, the cells were first thawed, pelleted (RT, 500 rfc, 5 min), washed with PBS and pelleted again before the protein extraction. More detailed protocol for this membrane protein extraction with RIPA buffer can be found in APPENDIX 3.

2.5 Optimising Western blot method

This project also included optimising the Western blot (WB) protocol to find the most suitable method for the Na_V subunit verification. The instructions form Alomone Labs ("Western blot analysis") were used as a reference. Optimising of WB was also executed with ARPE-19 cells.

The numerous SDS-PAGE runs during the WB optimising process were all completed similarly and changes with voltage and run time were tested. In addition, the protein transfer was carried out similarly throughout the whole project. Identical equipment, materials and gels were used in SDS-PAGE and protein transfer. SDS-PAGE was performed according to Laemmli (1970) under

denaturing conditions (4x Novex Bolt™ sample buffer, Cat# B0007, Life Technologies) on a 3-8% tris-acetate gel. SB and the protein lysates were combined in 1:3 ratio so that the total volume was 24 µl. Various temperatures for sample preparation were tested: boiling at 95-100°C, heating at 37°C and heating at 70°-85°C.

The pre-cast SDS-PAGE gel (3-8 % Tris-Acetate Gel, Cat# EA0375BOX, Invitrogen) was placed in Novex Bolt Mini Gel Tank (Invitrogen) and filled with 1x running buffer (Novex Bolt™, Cat# B0002, Invitrogen). The heated samples and pre-stained size ladder (PageRuler™ Plus, Cat# 26619, Thermo Scientific) were pipetted into the gel wells (V_{max} = 25 µl, $V_{standard}$ = 5 µl). SDS run was tested with 100-150V.

After the SDS-PAGE run, the proteins were transferred onto a nitrocellulose membrane. Protein transfer was executed with Bio-Rad Trans-Bolt® Turbo™ Transfer System and Trans-Blot® Turbo™ RTA Transfer Kit reagents (Mini-size 7.1x8.5 cm, 5x transfer buffer, transfer stacks, Cat#170-4270) were used according to the manufacturer's instructions. The transfer protocol used was optimised for high MW proteins were provided by the manufacturer (1.3 V, 25 A, 10 min).

After protein transfer, immunostaining of the nitrocellulose membrane was performed according to the instructions by Alomone Labs ("Western blot analysis"). Here, the background and unspecific biding of antibodies were blocked with 3 % BSA (Sigma-Aldrich) in 1x PBS + 0.1 % Tween-20 (Sigma-Aldrich) for five hours. Next, the membrane was incubated with the primary antibody overnight at +4 °C. The antibodies were prepared in blocking buffer (3 % BSA in PBS + 0.1 % Tween-20). During the optimising phase only $Na_V1.4$ subunit (Alomone Labs) was tested. Finally, after WB protocol optimisation was finished, also $Na_V1.5$ (Alomone Labs), $Na_V1.6$ (Alomone Labs), $Na_V1.8$ (Alomone Labs) and $Na_V1.4$ from other manufacturers (Abcam and Invitrogen) were stained. More detailed antibody information is presented in APPENDIX 1.

After the primary antibody incubation, the WB membrane was washed with wash buffer (0.1 % Tween-20 (Cat# P9416-50ML, Sigma) in 1x PBS, 3x 15 min). Next the HRP peroxidase conjugated secondary antibody (Abcam) was prepared in wash buffer (0.1 % Tween-20 in 1x PBS). The nitrocellulose membrane was incubated in the secondary antibody solution for 1h. The secondary antibody was washed 3x 15 min with wash buffer. Finally, the HRP signal was enhanced with chemiluminescence detection kit (ECL, Cat# K-12045-D20, Advansta) according to the manufacturer's instructions and immediately after this the membrane was visualised with Bio-Rad gel imaging instrument (Molecular Imager® ChemiDoc XRS + instrument). All washes and incubations were done at RT with gentle agitation if not mentioned otherwise. The more detailed Western blot protocol can be found in APPENDIX 4.

2.6 Molecular Weight analysis of the blots

The molecular weight of the visualised Na_V band were determined and calculated graphically from WB blots according to the instructions of Bio-Rad (Bulletin 3133). The migration measurements needed in these calculations were done based on figures 5-8 in APPENDIX 5.

The WB images obtained with the Bio-Rad gel imaging tool were analysed to estimate the molecular weights for each visible band. The size ladder in the images gives valuable information for the result analysis but it is merely an approximation. In addition, if there are multiple unidentified protein bands more accurate quantitative analysis of the MW of these bands is necessary (Bio-Rad Bulletin 3133). However, even these MW calculations are not absolute. Nevertheless, MW determination graphically might still be more accurate than just the visual comparison which is highly biased. The absolute MW values of the Na_V samples should, however, be determined with mass spectrometer. The calculations described below were executed for each WB image similarly.

For the graphical determination R_f values of size standard proteins bands needed to be defined. With Equation 1 the R_f value is determined when the migration distance of the size ladder protein through the gel divided by the migration distance of the dye front:

$$R_f = \frac{migration\ distance\ of\ the\ protein\ (mm)}{migration\ distance\ of\ the\ dye\ front\ (mm)} \quad (1)$$

First the distances of the size ladder bands were measured manually from the WB images and R_f values were calculated. The size standard MW values were turned into log MW values. An Excel chart and a standard curve were formed based on the R_f (x) and log MW (y) of the size ladder bands. Next, an equation of the curve was determined (Equation 2):

$$y = mx + b \quad (2)$$

where y is the log MW, m is the slope and x is the R_f. In addition, the linear relationship between the MW of the standard proteins and migration distance (R^2) was defined. With this value, the reliability of the MW predictions could be evaluated; if R^2 is > 0.99 the calculated molecular weights are reliable.

Next, the R_f value for the unknown sample band was determined similarly as for the size standard bands (Equation 1). The MW of the unknown bands were determined with Equation 3. MWs were calculated by inserting the R_f values i.e. x to the standard curve equation. When y = *log MW*, the molecular weight of the protein is:

$$y = mR_f + b \rightarrow MW = 10^y = 10^{mR_f + b} \quad (3)$$

The calculated molecular weights of the Na_V samples were then compared with reference sizes of the same sodium channel subunit. All the measurements, graphs, standard curves, tables and calculations of the molecular masses are assembled in APPENDIX 6.

3 RESULTS

3.1 Immunoassay and LSCM imaging

While imaging the immunofluorescent assayed iPSC-RPE samples not all Na_V subtypes were observed: $Na_V1.1$, $Na_V1.2$, $Na_V1.3$, $Na_V1.7$ and $Na_V1.9$ were not visible (Figure 1). In each sample however, the ZO-1 marker was detected .. Because these five subunits were not detected in the analysis, it was decided that these subunits would not be further extracted or examined in this project.

A

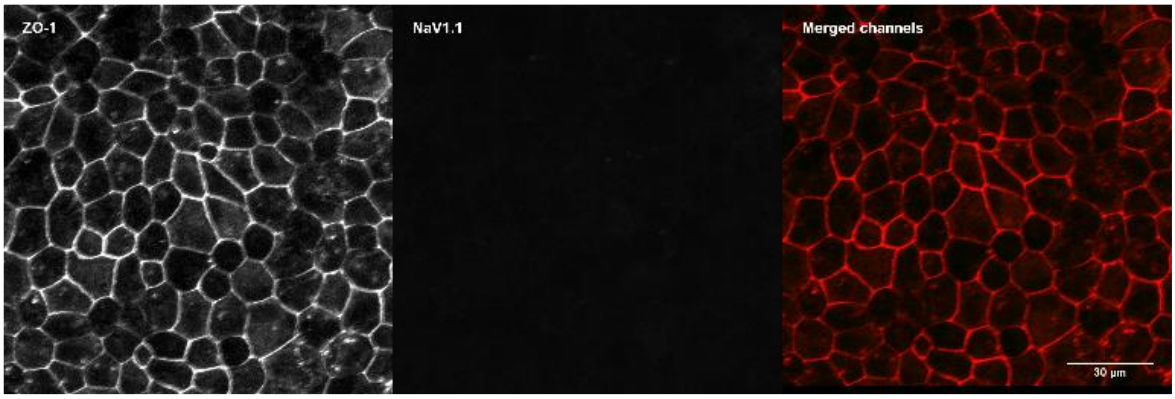

B

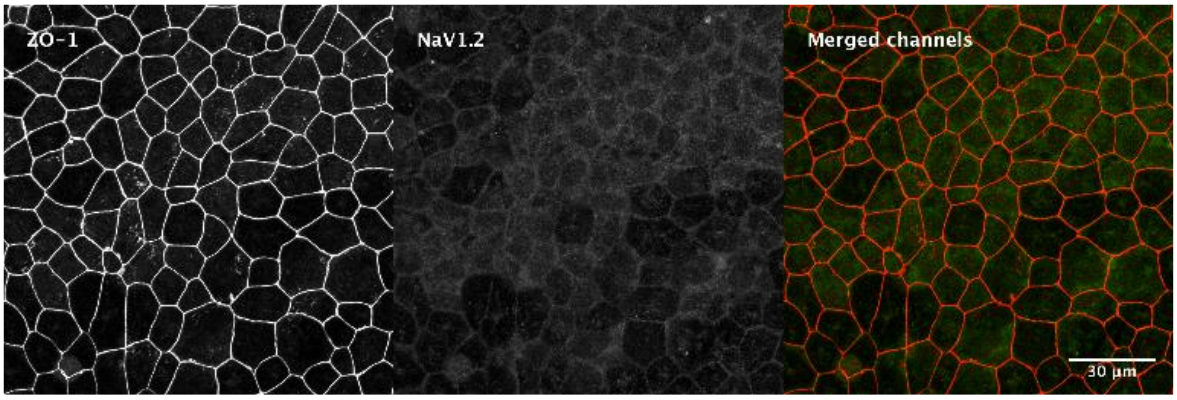

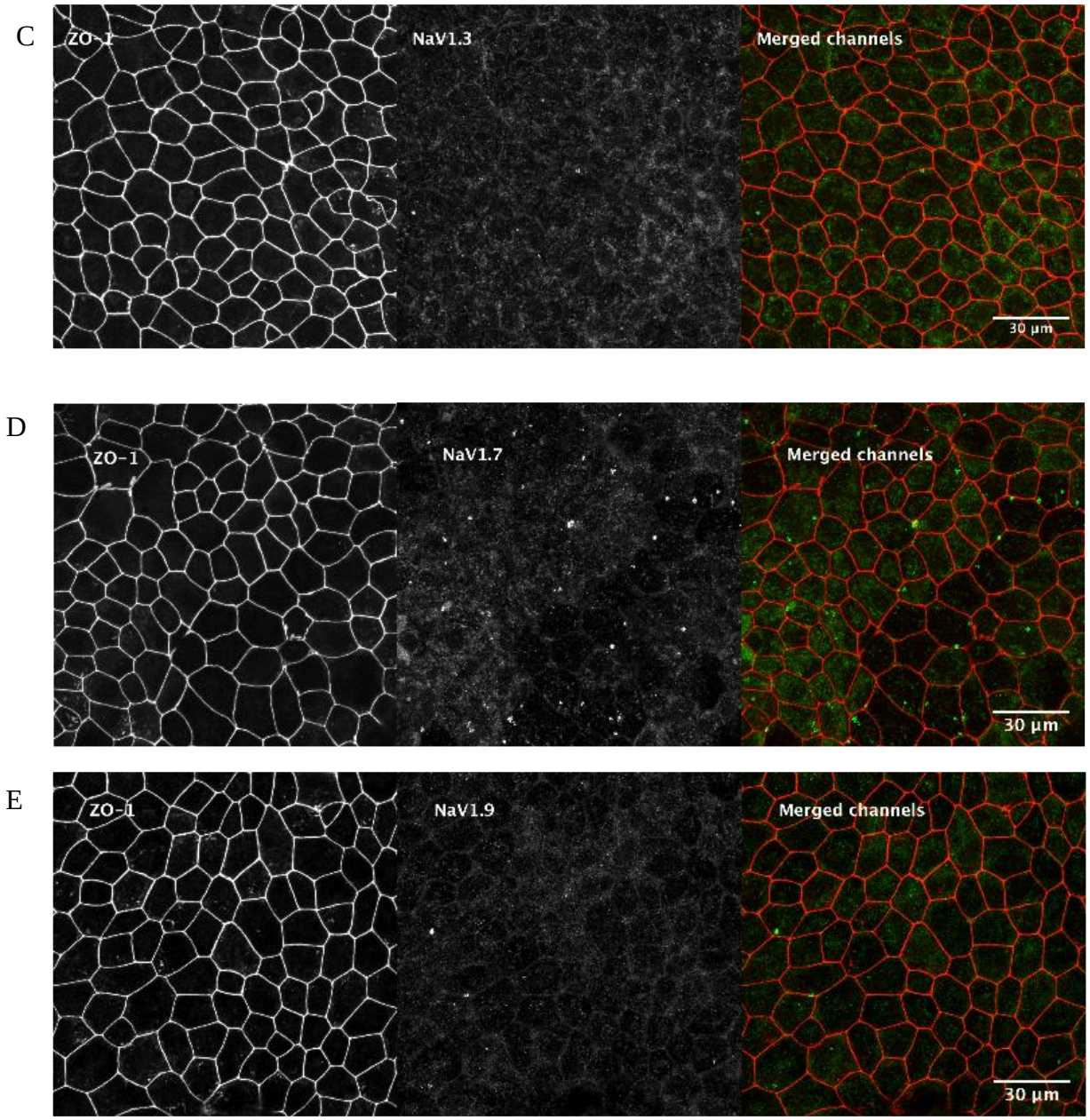

Figure 1. Microscopy images of the Na_V subunits that were not identified signals by immunolabeling. Subunits, A) $Na_V1.1$ B) $Na_V1.2$ C) $Na_V1.3$ D) $Na_V1.7$ and E) $Na_V1.9$. were not reliably detected from iPSC-RPE cells while examined with confocal microscope. In the three-picture panel the first image represents the tight junction protein ZO-1 second panel a specific Na_V subtype and the third image has both channels merged. ZO-1 was clearly visible in every sample. The images were produced with LSCM and images are shown as maximum intensity projections (MIP). The scale bar in each image is 30 µm.

Interestingly, positive labelling was observed from the samples stained with anti-$Na_V1.4$, anti-$Na_V1.6$, anti-$Na_V1.5$ and $Na_V1.8$ antibodies (Figure 2). The detected Na_V signals were clearly visible and brighter than with the previously mentioned Na_V subunits (Fig.1 A-E). In addition, the tight junction marker ZO-1 is apparent in each sample as well (Fig. 2A-D). These four detected Na_V subtypes were chosen for further analysis with the WB method.

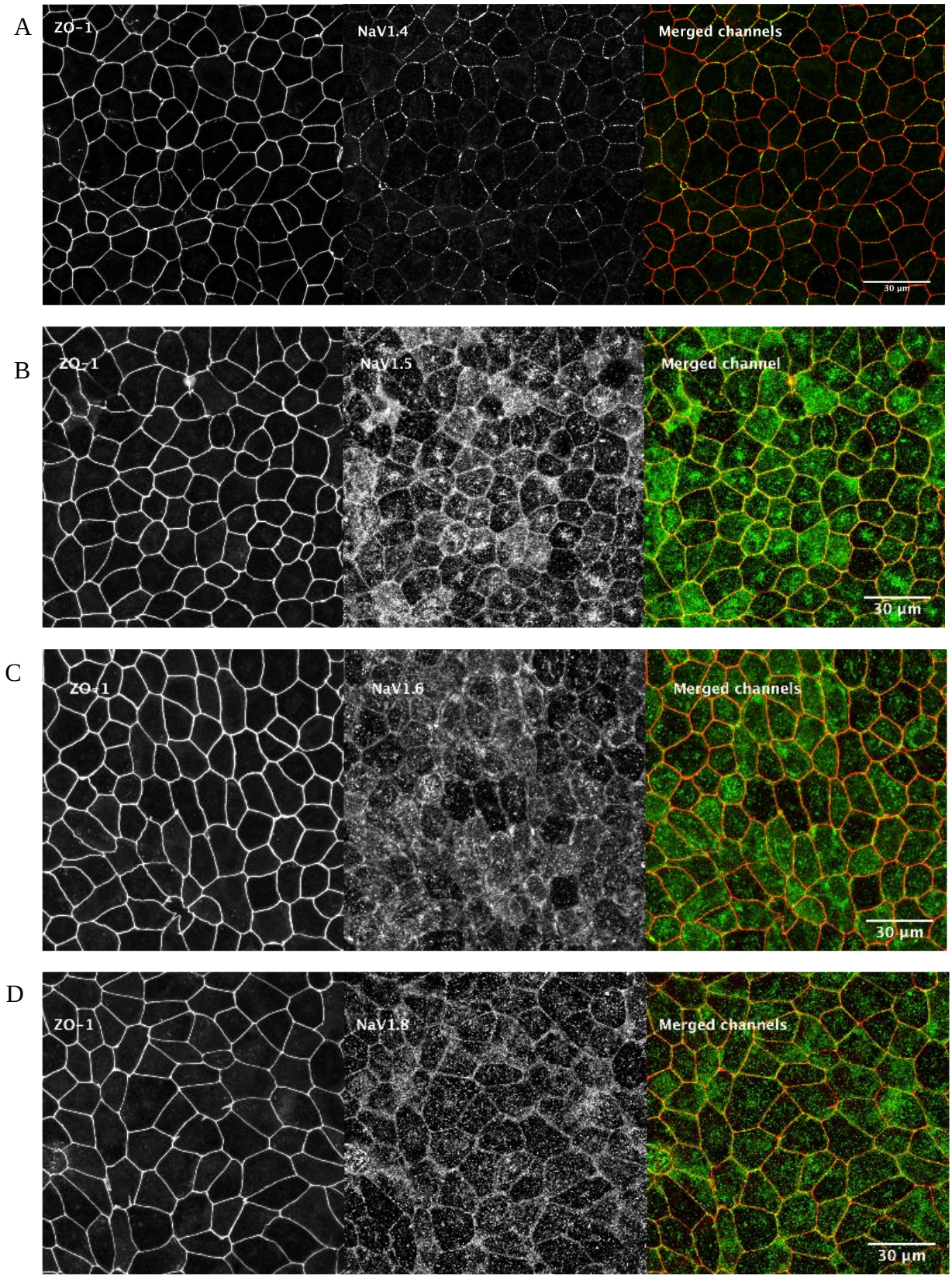

Figure 2. Microscopy images of the Na_V channel subunits which produced positive signal after immunoassays and imaging with LSCM. These immunoassayed Na_V

channel subtypes, A) $Na_V1.4$ B) $Na_V1.5$ C) $Na_V1.6$ and D) $Na_V1.8$. were clearly observed with confocal microscope from iPSC-RPE cells. In the three-picture panel the first image represents the tight junction protein ZO-1, second panel a specific Na_V subtype and the third image has both channels merged. These subunits were also chosen to be extracted and verified with WB. In the merged images the Na_V subunits are shown in green, the ZO-1 in red and possible colocalization between these two in yellow/orange. The scale bar in each image is 30 μm.

3.2 Na_V extraction and Western blot

Most of the tested membrane protein extraction methods were found to be inefficient and unsuitable for the purpose of this study. The commercial extraction kit, Laemmli buffer extraction (data not shown) and the Triton X-114 approach did not produce visible bands in the WB membranes. These methods were not pursued further in this thesis.

Isolation protocol based on instructions of Abcam combined with RIPA buffer was chosen to be used for the further experiments and optimisation. The results of the RIPA extraction and followed WB improved during the optimising process (Figure 3). However, the RIPA buffer alone did not yield detectable protein bands on the WB membrane in the correct size range (Fig.3A & B lanes 6-7). The Na_v channels labelling was found to be improved when the lysis buffer was supplemented with protease inhibitor cocktail and EDTA were not denaturised and (Fig. 3 B lanes 2-5 and C-F). Furthermore, the relevance of the sample buffer brand was revealed by testing two different SDS-PAGE sample buffers, 2x Laemmli (prepared in the lab) and commercial 4x Novex (Fig. 3B). The Novex SB (Fig. 3B lanes 4-5) produced higher resolution bands than the traditional Laemmli SB (lanes 2-3). SDS-PAGE run was optimised to start with 100 V (for the first 15 min), after which voltage was increased to 130V (for 10 min) and finally to 150 V (for 18-20 min). The total tun time was kept 43-45 min.

Early on it was clear that membrane protein samples should not be denaturised by boiling like soluble proteins but those should be heated instead. Different mild heating temperatures were tested to see which would be most suitable. In heating

experiment, protein lysates from a same batch were heated in 37 °C and in 75-80 °C for 10 min in sample buffer before loading them into the gel. In both cases the Na_V bands were quite faint but heating with higher temperature (75-80 °C) yielded in fewer bands and produced less background (Fig. 3E). The low heating temperature (37°C) resulted in great accumulation of protein aggregation in the gel wells and these proteins did not migrate in the gel properly during the electrophoresis which can be seen as the dark area at the top of the gel. Aggregation was less evident with the higher temperatures. After this experiment, lysates were heated at 70°C, because the proteins were denatured but aggregation was. In addition, when the temperature was decreased from 75 °C to 70°C the WB resolution improved. Therefore, it was decided that all membrane proteins extracted and analysed later in this study should be heated at 70 °C for 10 min.

The cause of the background was investigated with a peptide test to see if the dark background colour was due to unspecific binding of primary antibodies. The membrane strip incubated in antibody-peptide solution (Fig. 3C) did not produce protein bands, but the faint background was visible. Furthermore, background caused by the secondary antibodies was tested by incubating the WB membrane without primary antibodies (Fig. 3D). The nitrocellulose membrane strip incubated solely in secondary antibodies showed no background and only faint bands in non-Na_V size range.

After the optimising process, the Na_V bands were detected from the ARPE-19 lysates and importantly also from hESC-RPE samples (Fig. 3F). However, the bands were faint, so the antibody dilutions required additional optimisation.

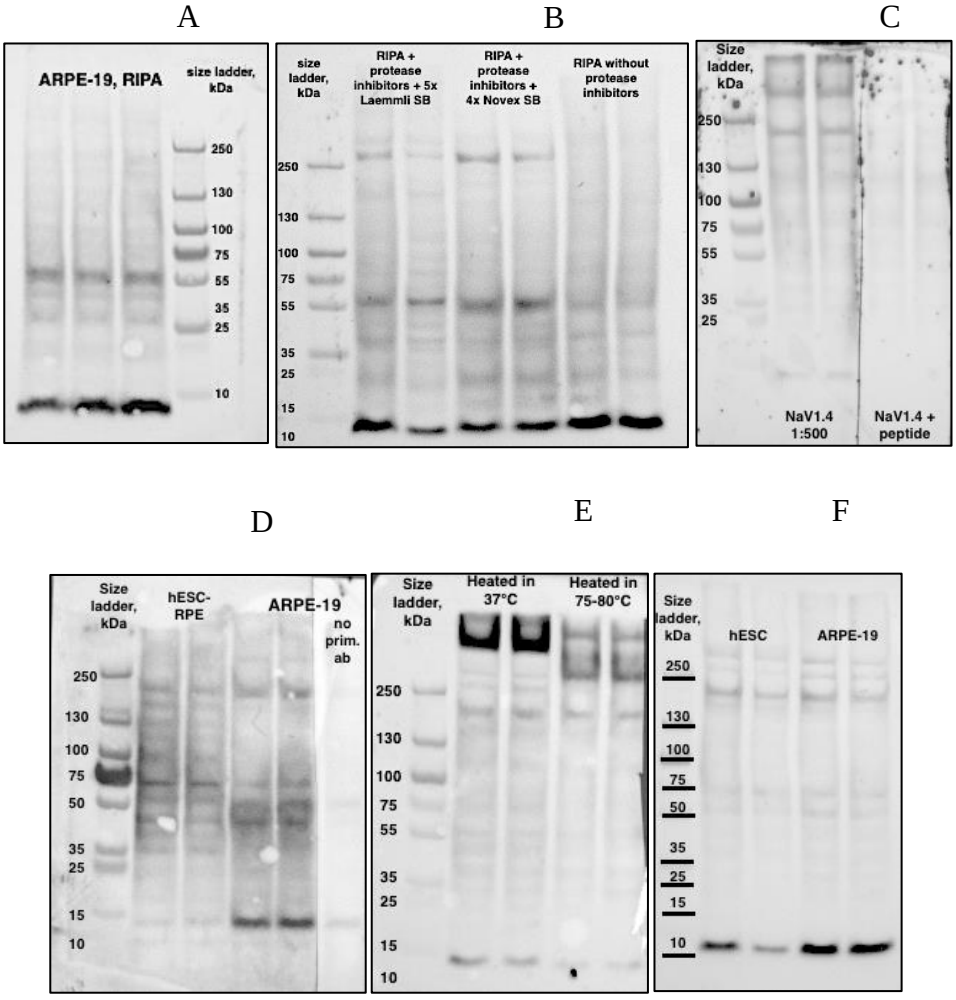

Figure 3. The process of optimising the protein extraction and Western blot method. All optimising tests were executed with anti-Nav1.4 primary antibody and HRP conjugated secondary antibodies, and the labelling was studied from either ARPE-19 or hESC-RPE lysates as indicated in the image. The dark bands at the bottom of each blot presented the sample and SB front, and these were not considered to be any actual result bands. A) RIPA extraction from ARPE-19 cells without the presence of protease inhibitors. No clear band was found in the 240-260 kDa area. B) RIPA extractions with protease inhibitors (lanes 2-5) vs. RIPA extractions without protease inhibitors (lanes 6-7). Clear bright bands in 260 kDa and 55 kDa area were formed with the samples which contained protease inhibitors. While the sample without protease inhibitors (lanes 6-7) did not yield any bands. Lanes 2-3 showed a sample with 2x Laemmli sample buffer and lanes 4-5 showed a sample with 4x Novex SB. C) Peptide test. The two-lane strip in the right (lanes 4-5) represented the part of the membrane which was incubated in solution consisting of primary antibody that was blocked with a suitable peptide. The other sample was stained without the peptide incubation (lanes 2-3). Bands with the correct size range were not identified in the peptide treated blot D) Secondary antibody test. The lane 6 showed a membrane strip which was incubated solely in secondary antibody

solution without primary antibody treatment. The other blot fragments were treated normally with primary and secondary antibodies (lanes 2-5). Minimal background was found to be caused by the secondary antibodies. E) SDS-PAGE sample heating test. The other ARPE-19 lysate (lanes 2-3) was heated for 10 min at 37 °C and the other lysate for 10 min in 75-80 °C (lanes 4-5). The 37 °C lanes showed faint background and protein bands but very dark area at the top of the membrane. The dark area represented the aggregated and accumulated membrane proteins which have not migrated through the gel during the electrophoresis. This type of aggregation was also seen in the lysate, which was heated at higher temperature, though the accumulation of the proteins seemed to be less evident and more scattered. F) Final WB results. The Na_V bands were visible in lysates obtained from both ARPE-19 and hESC-RPE cells though the bands are very faint. In addition, there were additional, visible but faint bands. The intensity of the apparent background signal was successfully decreased through the optimisation.

After the optimising processes the actual verification of the four Na_V subunits was initiated. Lysates from ARPE-10 and hESC-RPE created multiple bands in blots when stained with anti-Na_V antibodies (Figure 4). However, the brightest visible bands were found in the 130-250 kDa range. Uncropped WB images are presented in APPENDIX 4.

As mentioned before, the WB results are not absolute and only the visual determination of the molecular weights of the bands is insufficient. The quantification of the MWs was therefore needed (calculations in APPENDIX 5, results in Table 1). This ensured the proper evaluation of the Western blot images. In all the WB images the aggregation of the membrane protein is detectable as a dark band-like area on top of the blot in each lane.

Anti-$Na_V1.4$ revealed two bright bands in the 150-200 kDa range (Fig. 4A). Molecular weight determination revealed that the first band (215 kDa) is more consistent with the reference MW of $Na_V1.4$ (208 kDa). However, the second band is not in the $Na_V1.4$ size range of 185 kDa (Table 1). The reference molecular weights were obtained from the antibody manufacturer (Abcam) and from UniProt database. Both references suggest the same molecular weight for the $Na_V1.4$ subunit, which is 208 kDa. Similarly, the first band (196 kDa) in $Na_V1.5$ WB

membrane (Fig. 4B) is more consistent with the reference molecular weights (220-227 kDa, Alomone Labs and Uniprot database, Table 1) than the second band (162 kDa). Both $Na_V1.5$ bands had the same resolution and intensity.

In the $Na_V1.6$ WB membrane there were two detectable bands (Fig.4C): one very faint band which was more consistent with the $Na_V1.6$ reference MW (220 kDa, Table 1) and a clear, bright band which was only 154 kDa (graphically determined MW, Table 1). The first band was more evident in the ARPE-19 samples. The smaller i.e. the bright band differs from the suggested $Na_V1.6$ isoforms, but it resebled the size of the $Na_V1.6$ isoform 4 (145 kDa, UniProt).

The $Na_V1.8$ created multiple faint protein bands in the membrane (Fig 4D). There are three distinct and brighter bands visible, but only one of these bands is in the correct size range, the first brighter one, which is 198 kDa (Table 1). There are also two obscure bands above and below the 198 kDa band: 240 kDa and 171 kDa though these two are only barely visible.

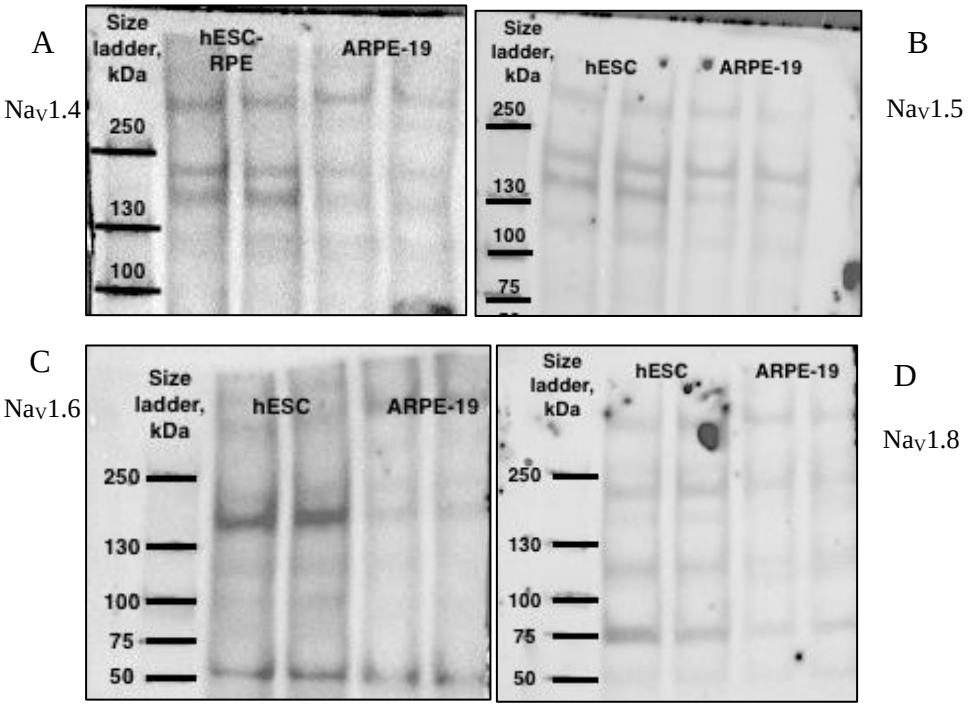

Figure 4. Final Western blot results. In all four images (A-D) the first lane represented the size standards, lanes 2-3 were membrane proteins samples isolated from hESC-RPE cells and lanes 4-5 represented the lysates from ARPE-19 cells. The bands on top of each lane (>250 kDa) represented the section from which the proteins entered to the gel. These bands were not considered to be a result to interpret, but merely the aggregated membrane proteins which did not migrate through the gel during electrophoresis. These images are cropped to highlight the Na_V bands, the original uncropped images are presented in APPENDIX 5. A) $Na_V1.4$. There were two visible bands on the blot. According to the MW calculations the first, band was 215 kDa whereas the second band was 185 kDa (reference size according to manufacturer was 208 kDa). B) $Na_V1.5$. There were two visible bands with similar intensity intensity. The MW determination revealed that the size of the first protein is 196 kDa and the second was 162 kDa (reference size for $Na_V1.5$ is 220 kDa). C) $Na_V1.6$. The anti-$Na_V1.6$ revealed very faint, barely visible 220 kDa band and a very bright 154 kDa band which corresponded to the size of $Na_V1.6$ isoform 4 (145 kDa) D) $Na_V1.8$. In this blot there were clearly more protein bands than in other membranes; there were few brighter bands and two very faint bands visible. The largest MW band was in the $Na_V1.8$ reference size range as it was 198 kDa. There were also 240 kDa and 171 kDa bands which were barely visible though in the membrane.

Table 1. Graphically determined molecular weights of the unknown protein bands in the WB membrane. The MWs of most significant bands were defined and calculated. In each row, the reference MW of each Na_V subunit was shown. Calculations based on the measurements gotten from images are shown in APPENDIX 5. The images on which the measurements were based on are presented in APPENDIX 4. The reference sizes were based on the information of the antibody manufacturer as well as the from the protein database UniProt. In the protein database also the possible subtype isoforms and their sizes were introduced.

Na_V subunit	**Graphically determined MW**	**Reference MW**	**Reference MW origin**
$Na_V1.4$	1° Band 215 kDa 2° Band 185 kDa	208 kDa	Abcam Uniprot
$Na_V1.5$	1° Band 196 kDa 2° Band 162 kDa	220-227 kDa (Isoforms 1-6)	Almone Labs Uniprot
$Na_V1.6$	1° Band 220 kDa 2° Band 154 kDa	220-226 kDa (Isoforms 1-3, 5) 145 kDa (Isoform 4)	Alomone Labs Uniprot
$Na_V1.8$	1° Band 240 kDa 2° Band 198 kDa 3° Band 171 kDa	220 kDa 170 kDa	Alomone Labs Uniprot

4 DISCUSSION

Immunocytochemistry and LSCM imaging revealed that RPE Na_V channels, spefically the subtypes $Na_V1.4$, $Na_V1.5$, $Na_V1.6$ and $Na_V1.8$ are present in RPE and they colocalize with ZO-1 (Figure 2). This suggests that Na_V channels would be located near the tight junctions. Especially $Na_V1.4$ signal was clearly restricted in the plasma membrane and colocalised perfectly with ZO-1. However, positive cytosolic signals were also detected when observing the $Na_V1.5$, $Na_V1.6$ and $Na_V1.8$ samples, which might indicate unspecific binding of the primary anti-Na_V antibodies or background caused by the secondary antibodies. Alternatively, because the cytosolic signals in these three samples were brighter than in any other sample, they might originate from the cytosolic membranes e.g. ER or transportation vesicles. These findings were interpreted to indicate that at least $Na_V1.4$, $Na_V1.5$, $Na_V1.6$ and $Na_V1.8$ subtypes are present in RPE. These channels were then chosen to be analysed from RPE cells lysates with WB.

The subunits $Na_V1.1$, $Na_V1.3$ and $Na_V1.7$ were not detected from the immunoassayed cell samples (Figure 1) despite the fact that ZO-1 labelling was evident in all of the samples. The lack of signal might indicate that these Na_V channel subtypes are not present in the RPE. When observing the images of $Na_V1.2$ and $Na_V1.9$ in both images there was a very faint signal pattern which colocalized with the ZO-1 marker. This pattern was clearer in these two images compared to the other subunits that were left outside of the further experiments. This finding could indicate that RPE might express also these two subtypes. If these two would be expressed in the RPE they could be less abundant, that could explain the weak signal. Other explanation could be that the antibodies used did not bind the target protein sufficiently enough to be properly detected. The specificity and efficiency of the used antibodies could be tested by changing the manufacturer of the antibody. This could also apply to other undetected subunits as well. So, the undetected subunits could be re-examined with alternative antibodies or techniques as well as the subunits $Na_V1.2$ and $Na_V1.9$. It was still concluded that these five Na_V subunits

should not be further examined or extracted at this point because it seemed that these proteins were not abundant in RPE cells.

Interestingly, Johansson et al. (2019) did prove that at least subunits $Na_V1.1$, $Na_V1.3$-1.9 are presence in the RPE. Therefore, it seems that the negative results obtained from the LSCM were false negative results. This in turn might be due to flaws on the staining protocol. However, the protocol used in this project was the same as the one used in the study of Johansson et al (2019). The only differences were the cell types and the fixing method used: Johansson et al. (2019) used mouse RPE cells and hESC-RPE cells and fixed their cell samples with 4% PFA. So, the methods used here could be slightly flawed or there might have been trouble with the protocol execution. The similarity with the immunocytomertry and imaging protocols could also suggest that the Na_V channels might be less abundant in iPSC-RPE than in hESC-RPE, or that the methanol might affect the Na_V channels in a way that results in undetectable or very faint signal. Findings of Johansson et al. (2019) prove that the rest of the subunits would have required more examination even in this project.

Though the microscopy images indicated the presence of the Na_V subunits, these results needed to be verified. This required isolation of the target membrane proteins and their detection with WB. These methods in turn required planning, background research and optimisation.

Different condition and treatment tests helped to construct the final protocols. Of the tested extraction methods, isolation with RIPA lysis buffer combined with protease inhibitor cocktail and EDTA yielded most optimal results. The content of the RIPA lysis buffer used in this project was similar as the one recommended by MacPhee (2010) but instead of TX100 Nonidet P-40 (NP-40) was used. Between these two reagents, there should not be any differences in isolation results, but NP-40 is modestly gentler (MacPhee 2010). The other tested membrane protein procedures did not produce any results in this study. This might be due to poor separation of the soluble proteins and membrane proteins, aggregation of the membrane proteins

or significant protein loss during separation process. Alternatively, these methods might fail to efficiently cleave the membrane proteins from their native environment. All these issues can lead to faint or non-existent protein bands. As a result, all the other methods were rejected, and experiments were carried out solely with the RIPA lysis buffer.

Despite the fact that protein isolation was most successful with RIPA buffer, in all the WB images the aggregation of the membrane protein is detectable as a dark band-like area on top of the blot in each lane. These are most likely the extracted membrane proteins, which did not enter the gel during gel electrophoresis due to aggregations which membrane proteins form very easily. This in turn seems like the sample preparation might need improvement.

Heating tests revealed that boiling or heating at low temperature, at 37 °C, is not suitable for these membrane proteins. Quick heating in 70 °C seem to be the best way to denaturise Na_V proteins without aggregating them too much. Heating the membrane protein samples at 90°C or above can lead to considerable aggregations and other problems (Schagger 2003). The membrane protein lysates should not be boiled but actually incubated in lower temperatures, e.g. at 40°C for 30 minutes (Schagger 2003). One reason why heating at lower temperature was so unsuccessful could be the SB used, which is optimised to work at 70°C (10 min). This was also the temperature that produced the best results.

While testing the extraction protocol with RIPA lysis buffer it became evident that Na_V channels are especially vulnerable for degrading effects of the proteases which emerge during cell lysis. The results of this study suggest that when proteases are not inhibited, the Na_V channels are completely decomposed and are not detected with WB (Figure 3A and B). Moreover, the addition of EDTA was shown to improve the WB resolution, because it prevents target protein lysis (Ohlendieck 1996, Von Jagow et al. 2003).

The peptide test was executed to test whether the signals in the background in microscopy images or dark colour of the blots were due to unspecific binding of the primary antibodies. Peptide tests showed that the background caused by the primary was not significant (Figure 3C). Testing the secondary antibodies for dark background in WB revealed that they do not cause the dark background either, and unspecific binding was not detected. Therefore, these two tests indicate that the antibodies themselves might not be the cause of dark background in WB. However, in the peptide test, only anti-Na_V was tested with blocking peptide. It could be beneficial to check other antibodies with this type of test as well.

MacPhee has noted that high background is usually due to inefficient washing of the membrane and not necessarily due to antibodies (MacPhee 2010). This could be the case in this study though the washing steps were kept quite long (15 min each). Sometimes the antibody concentrations are too high or the antibody incubation conditions (temperature and time) are not optimal and therefore cause dark background. These possibilities, however, can be ruled out as the WB protocols and conditions were optimised here and similar methods were also used in the research of Johansson et al. (2019).

Other possible causes of dark background are usually caused when primary or secondary antibody binds to the blocking agent (e.g. BSA), non-specific interaction between antibodies and leftover genomic DNA in samples, insufficient blocking or over exposure while imaging the membrane ("Western Blot Troubleshooting"). Alternative solutions to reduce these high background sources could be to use alternative blocking buffer (e.g. milk based), reducing protein concentration of blocking agent, addition of DNAse into the lysis buffer, alternative blocking temperature or diluting ECL solution ("Western Blot Troubleshooting", accessed 2020).

The SDS-PAGE run was noted to produce good results when the voltage is low, 100 V, but unfortunately slow protein separation reduces band quality (Schagger 2003).

However, too high voltage reduces the WB resolution, creates blurry bands and the dye front might not proceed straight ("Western Blot Troubleshooting", accessed 2020). So, by starting the run with 100 V and then by increasing the voltage first to 130V and then to 150V ensured steady sample entering into the gel, even movement of the proteins, protein separation and good WB resolution.

During optimising it was also noted the long blocking period (at least 5h at RT) used in the immunoblotting protocol reduced the amount dark background and improved the results. Usually blocking of the WB membrane is executed because it may block any potential non-specific binding sites on the membrane itself, but longer blocking time can also promote antigen retrieval and therefore enable specific antibody binding (MacPhee 2010). Johansson et al. (2019) also used the five-hour incubation in their study.

After the optimisation efforts, a successful protocol was established to analyse integral membrane proteins from cultured RPE cells. The Western blot results and the calculated molecular weights of the unknown protein bands were comparable to the data obtained with immunocytochemistry: the Na_V subunits 1.4, 1.5, 1.6 and 1.8 were identified in RPE (Figure 4). Moreover, these subunits could be verified in hESC-RPE with WB. Nonetheless, WB results revealed some additional information about these Na_v channels and raised some questions: why are there multiple visible bands in the blots and why do the visible bands seem to differ in size from the sizes reported in literature? And why are the detected Na_V bands are so faint?

According to Bio-Rad ("Western Blot Troubleshooting") additional or bands with different size than expected can be caused by variety of reasons: cleaved or digested target protein, existing protein isoforms, dimers, multimers and unexpected protein-protein interactions or cross-reactivity with same or similar epitope on other proteins has been detected with the same antibody used. These issues can be solved by additional protein or protease inhibitors, reducing agents (such as DTT), alternative antibodies (another manufacturer), a peptide test or preparing a new

lysate ("Western Blot Troubleshooting", Bio-Rad). Moreover, according to the "Western Blot Troubleshooting" (Bio-Rad) weak signals from the bands might be due to low antigen binding affinity, insufficient sample loading on the gel or low antibody concentration. Because the antibody concentrations were optimised, and similar methods and antibody dilutions were also used by Johansson et al. (2019) this probably was not the case here. Weak bands could be improved by reducing wash steps or duration, concentrate the sample protein or increase the source material.

According to literature the mammalian Na_V channels are approximately 260 kDa (Catterall 2000, Yu and Catterall 2003) but according to the antibody manufacturers and UniProt protein database the channel sizes range between 170-220 kDa (Table 1). According to Schagger (2003), the apparent molecular weight in WB membrane may differ from the actual, native protein size, because membrane proteins show abnormal migration behaviour in the SDS gels, might bind an unusual ratio of SDS molecules per amino acid residue or some hydrophobic peptides may not completely unfold during denaturation. This could explain some of the differences between the reference molecular weights, but not entirely. The dye front had proceeded uniformly, so the error of the MW determinations and calculations should be minor. The multiple bands raise question about the success of the extraction and WB. Yet, all the bands seem to migrate somewhat to the correct size range, when comparing the results with the reference sizes, $Na_V1.6$ being an exception with the bright 150 kDa band. The multiple bands might be, for example, due to a decomposing of the protein during heating. If the multiple bands are in fact degenerated parts of the Na_V polypeptide, it would mean that even after decay the Na_V antibody binding site should remain intact.

One other explanation for the additional bands could be that the RPE cells express different types of Na_V subunits, i.e. there are multiple isoforms of the same proteins. UniProt protein database e.g. describes six isoforms and seven potential isoforms for $Na_V1.5$, five isoforms and four potential isoforms for $Na_V1.6$ and one confirmed

isoform and two potential isoforms for $Na_V1.8$ produced by alternative splicing. $Na_V1.4$ has only one confirmed isoform and no reported potential isoforms.

Many eukaryotic genes encode more than one separate protein isoforms (Ahmad et al. 2012). Alternative splicing of the pre-mRNA transcripts can generate multiple mRNAs and hence create multiple different proteins from the same gene (Ahmad et al. 2012). Isoform proteins can vary in size, amino acid sequence, number and consistent of exons (Ahmad et al. 2012). In addition, about 40-60 % of human genes have alternative isoforms and roughly 30% of these alternative spliced genes are involved in signalling and regulation (Modrek and Lee 2002). Even many of the Na_V channels possess alternative splicing sites and some subtypes have different isoforms of different sizes (Black and Waxman 2013).

The alternative splicing model could explain why there are multiple bands detected in WB membranes: if the cell produces multiple Na_V isoforms which are different sizes, this could show in the blot as multiple bands. Because there are observations of Na_V channel isoforms in other cell types, it is quite possible that RPE could express multiple Na_V isoforms as well. In the case of $Na_V1.4$ the larger 215 kDa protein band most likely is the so-called correct $Na_V1.4$ band. The second, smaller band (185 kDa) could either represent decomposed $Na_V1.4$ protein, an unidentified isoform or a protein with unspecific bound anti-$Na_V1.4$ antibody caused by the antibody type/manufacturer. The primary antibodies should be epitope and protein specific, there might be differences between manufacturers with the binding and even between manufactured batches. Primary antibodies can sometimes also bind non-target proteins with similar or same epitope ("Western Blot Troubleshooting", accessed 2020).

The larger (196 kDa) of the two $Na_V1.5$ bands resembles more of the reference proteins than the smaller one (162 kDa). However, the $Na_V1.5$ lanes were not completely straight, and the dye front was slightly slanted so there might be some error in the calculations and the MWs might contain some error as well. Just like in

the case on $Na_V1.4$, the extra 162 kDa band might be an unidentified isoform or decomposed Na_V polypeptide part. The anti-$Na_V1.5$ manufacturer Alomone Labs also predicts that this antibody might create a broad band around the 220-260 kDa area with a faint band around 150-160 kDa or a single 200 kDa band. The antibody related staining pattern would explain the multiple bands. However, because the staining pattern of the antibody seems to be quite unclear, it is hard to evaluate the $Na_V1.5$ extra bands.

The faint, barely visible $Na_V1.6$ band was 220 kDa, i.e., the isoform that the antibody manufacturer is referring to and how large the most of the $Na_V1.6$ isoforms are. However, the very bright, broad band is only 150 kDa, which actually differs greatly from the Na_V molecular weights reported in literature. Could this significantly smaller protein band represent a $Na_V1.6$ isoform of some sort, for example the isoform 4 (145 kDa)? This theory is further supported by Plummer and others (1997 and 1998): The $Na_V1.6$ encoding gene SCN8A, consists of 1980 amino acid residues and it has two alternatively spliced exon pairs, exons 5N and 5A, and exons 18N and 18A (Plummer et al. 1997, Plummer et al. 1998) of which the exon 18 is more interesting regarding this project.

The alternative spliced exon 18N results in a shortened two-domain protein instead of four domains, and it is roughly 40% shorter than the full-length channel protein (Plummer et al. 1997). Plummer and others (1997) noticed that18N predominates at early embryonic stages, in fetal brain and in all of the non-neural tissues they tested. Plummer et al., (1997) also discussed that the SCN8A transcript 18N would not produce a functional Na_V channel as the protein is not full-length and therefore might not be active. Because the two-domain $Na_V1.6$ isoform is significantly shorter in sequence and smaller in size, the smaller 154 kDa band in WB could represent this $Na_V1.6$ isoform. Moreover, as the $Na_V1.6$ alternatively spliced form 18N is expressed in non-neuronal cells it could very well be expressed in RPE as well. This would explain why the smaller protein band is much brighter than the 220 kDa

isoform band; RPE could be one of those tissues where the two-domain $Na_V1.6$ isoform is the dominant form and much more abundant than the "normal" protein.

In this study, the WB results of the $Na_V1.8$ were most ambiguous. As it showed multiple faint bands and no significantly bright ones. These all seemed to set in the correct size range of $Na_V1.8$, and each them could actually indicate the correct Na_v channel There are three confirmed $Na_V1.8$ isoforms (UniProt database) but the molecular weight of these ranges between 220-221 kDa. On the other hand, the anti-$Na_V1.8$ manufacturer (Alomone Labs) states that their $Na_V1.8$ antibody does create two distinct bands in WB: one about in the 220 kDa area and one in the 170 kDa area. This indicates that the 171 kDa band would be a part of the staining pattern of the primary antibody and not an artifact or a contaminant. Nevertheless, these findings do suggest that $Na_V1.8$ is also found in RPE but this could not be confirmed as strongly as the other subunits, and this subunit requires some additional work to yield better WB results. The optimised WB protocol might not be suitable for this protein, so alterations should have been made accordingly. Johansson et al. (2019) had resolved the problem with $Na_V1.8$ by altering the WB: they blocked the membrane over night at +4°C, incubated the primary antibodies at RT for 1h and washing steps were only 10 min. These alterations produced better results in Johansson's et al. (2019) study. Subunit $Na_V1.8$ could be expressed in lower levels than the other channels and therefore it is harder to produce clear and bright bands of it in WB.

The multiple bands at least the faint ones could also be the result of unspecific binding of the antibody. They might be visible because the concentration of the proteins of interest is low: there is always some portion of background and unspecific binding while performing WB, which might not be visible if the bright signal of the target protein overpowers the brightness which originates from the unspecifically bound proteins. Conversely, if amount of the protein of interest is low the background and unspecific proteins seem relatively brighter because the signal from the actual target proteins is weaker and doesn't overpower the signal of

the false proteins. Low abundancy of the membrane proteins in cells usually results low quantity in cell lysates which further weakens detective signals in blots or gels (Santoni et al 2000).

When evaluating the Western blot results it should be remembered that this is an important tool in the field of protein research, because the specific binding of antibodies to the protein of interest permits sensitive and highly specific detection (Von Jagow et al. 2003). Yet this method has its flaws when studying membrane proteins. During electrophoresis, membrane proteins show unusual migration behaviour in the SDS gel and they can bind an unusual ratio of SDS molecules per amino acid residue (Schagger 2003). In addition, even in the presence of detergents and with optimised sample preparation conditions, membrane proteins can form aggregates and some of the very hydrophobic regions in the proteins may not completely unfold and enter the gel (Schagger 2003). These factors may alter the apparent molecular weight in gel and in WB membrane which therefore might differ from the referred concentration and size (Schagger 2003). This would explain why the graphically determined molecular weights of Na_V subtypes were not consistent with the referred MWs.

Further issues with WB lie with the actual protein detection: after antibody staining it is hard to proof that the detected signals from the blots are the proteins of interest rather than contaminants or protein parts (Santoni et al 2000), which was also noticed here. Moreover, compared to soluble and cytosolic proteins, the resolution of membrane protein bands in SDS gels and WB is generally weaker and the bands broader (Schagger 2003). This explains why the resolution of the bands was so weak.

These issues proof that WB solely is not the most reliable or precise tool when verifying and identifying unknown membrane proteins, peptides and isoforms from a protein lysate (Ahmad et al. 2012, Schagger 2003). Therefore, mass spectrometry should also be used to reliably identify proteins from lysates, but this

technique requires thorough lysate purification (Rigaut et al. 1999, Speers and Wu 2007, Wu and Yates 2003).

Despite the flaws in the WB method, the results obtained with this technique do seem to confirm that channel subtypes $Na_V1.4$, $Na_V1.5$, $Na_V1.6$ and most likely $Na_V1.8$ are present in RPE. However, the multiple bands in each blot remain mysterious. Also, the calculated MWs of the Na_V subunits do differ from the references, information of the antibody manufacturers and databases. Even though, there is a possibility of an error, the calculated and graphically determined MWs are still more reliable than just the images themselves.

Even though a successful protocol for membrane protein WB analysis was established during this study some issues were observed and therefore some modifications could produce even better results.

The first step to improve the WB results obtained here would be to increase the quantity of membrane proteins extracted from hESC-RPE. Because membrane proteins are not abundant in cells, increasing the cellular mass from which the membranes ought to be isolated is necessary. This might be a rather difficult task as the hESC-RPE cells are not easy to expand, or at least the expanding process would be very laborious. This is because, as mentioned before, after differentiation RPE does not usually renew itself and therefore passaging is not an option. Nonetheless, the more cell material there was available in the isolation process, the better membrane protein yield would be and accordingly the SDS-PAGE and WB would produce better results. In addition, large quantity of proteins ensures that the signal of the studied proteins compensates for the possible unspecific binding of antibodies and background.

Unlike in the protein structure determination studies or mass spectrometry analysis, here, the proteins were not purified after extraction. The membrane proteins were simply separated from the soluble material and cellular debris. Different purification methods such as simple filtration (e.g., commercial centrifuge

filters), gel filtration, ion exchange and affinity chromatography all remove impurities efficiently. Additional purification methods are essential if the goal is to analyse protein lysate with MS, but removal of detergent and other debris can also improve the WB results. However, additional purification steps always cause loss of protein and increase the chance of membrane protein aggregation, and even the simple filtration decreases the quantity of the protein, which would result in the increase of the starting material. This was one of the reasons why it was decided that these protein lysates were not further purified to save as much of the valuable proteins as possible. Therefore, it was decided that sufficient results could be obtained without protein purification. Johansson et al. (2019) succeeded to purify the sample for MS from SDS-PAGE gel and with vacuum concentrator to minimise protein loss.

Another option to improve the WB results, would be to screen antibodies from other manufacturers to compare the background, unspecific binding and protein band resolution. At least the improved differences between two antibodies were noted in the case of $Na_V1.4$: the optimising of the WB was initiated with Alomone Lab's antibodies and during the process, but it was noticed that Abcam created better results. Additional improvement operations could be to add reducing reagent to the lysis buffer or to use more sensitive ECL kit.

Further experiments should also contain membrane protein isolation and Na_V examination from primary tissue obtained from e.g. mouse eyes. Cell models are very useful and often the only way to examine some features but studying the native tissue would be useful and beneficial. Following experiments should also involve further examination of the other Na_V subtypes as well.

RPE research is crucial for understanding diseases which lead to blindness. Exploring the Na_v channels in the RPE could give rise to new discoveries about disease mechanisms or causes of ADM and maybe even help to find cures to retinal degeneration deceases.

This study verified the existence of four Na_V channel subunits in RPE, $Na_V1.4$, $Na_V1.5$, $Na_V1.6$ and $Na_V1.8$. These subtypes were detected while imaging immunoassayed iPSC-RPE cells with LSCM. Isolation of these membrane bound proteins was also successful with the RIPA buffer-based lysis protocol. Further, all extracted Na_V subunits were examined and detected with Western blot method, though the $Na_V1.8$ verification will require some additional work and improvement. In addition, the $Na_V1.6$ channel band observed in WB strongly correlates with the MW of a truncated, two-domain isoform that is predominant in non-excitable tissues. This could indicate that the $Na_V1.6$ subtype expressed in the RPE could be significantly smaller in size and in fact the correspond to the smaller isoform 4. The future studies will reveal more interesting features and details about the purpose of Na_V channel of the RPE. Verifying the presence of the Na_V channels is a first step exploring/studying the significance and roles of these channels in RPE.

ACKNOWLEDGEMENTS

This Master's research project was executed in Tampere University, in the Faculty of Medicine and Health Technology. The study was a part of the Doctoral thesis research of MSc. Julia Fadjukov (Johansson) in the Biophysics of the Eye group led by Dr. Soile Nymark. This work was supported financially by Tampere University (form. Tampere University of Technology. My internship and orientation prior to this study were enabled by the grant of Emil Aaltonen Foundation.

I would like to thank my supervisors and mentors Soile Nymark and Julia Fadjukov (Tampere University, form. Tampere University of Technology) for their guidance and support during this project. Big thanks to Taina Viheriälä for providing me the cells for the extraction experiments. I would also like to thank Teemu Ihalainen (Ph.D, Tampere University) for support and aid, and the lab technicians Ulla Kiiskinen and Niklas Kähkönen (Vesa Hytönen, prof., PhD, Protein Dynamics research group, Tampere University) for their practical aid. In addition, my thanks to the whole personnel in the Biophysics of the Eye group for their support and encouragement.

REFERENCES

Ahern C.A., Payandeh J., Bosmans F. & Chanda, B. 2016. The hitchhiker's guide to the voltage-gated sodium channel galaxy. J. Gen. Physiol. Vol. 147 No. 1 1–24. doi: 10.1085/jgp.201511492.

Ahmad Y., Boisvert F.M., Lundberg E., Uhlen, M. & Lamond A.I. 2012. Systematic Analysis of Protein Pools, Isoforms, and Modifications Affecting Turnover and Subcellular Localization. Molecular & Cellular Proteomics 11:1–15. doi: 10.1074/mcp.M111.013680.

Anti-NaV1.5 (SCN5A) Antibody, Cat# AGP-008. Alomone Labs. https://www.alomone.com/p/anti-nav1-5-2/AGP-008 (accessed 11/2020)

Anti-NaV1.6 (SCN8A) Antibody, Cat#ASC-009. Alomone Labs. https://www.alomone.com/p/anti-nav1-6/ASC-009 (accessed 11/2020)

Anti-NaV1.8 (SCN10A) Antibody, Cat# AGP-029. Alomone Labs. https://www.alomone.com/p/anti-nav1-8/AGP-029 (accessed 11/2020)

Anti-SCN4A antibody (Cat# ab65165). Abcam plc. https://www.abcam.com/scn4a-antibody-ab65165.html (accessed 11/2020)

Black J.A., Newcombe J. & Waxman S.G. 2013. Nav1.5 sodium channels in macrophages in multiple sclerosis lesions. Multiple Sclerosis Journal 19(5) 532–542. doi: 10.1177/1352458512460417.

Black, J.A. & Waxman S.G. 2013. Noncanonical Roles of Voltage-Gated Sodium Channels. Neuron 16;80(2):280-91. doi: 10.1016/j.neuron.2013.09.012. PMID: 24139034.

Bok D. 1993. The retinal pigment epithelium: a versatile partner in vision. J. Cell Sci, Supplement 17, 189-195. doi: 10.1242/jcs.1993.Supplement_17.27.

Bordier C. 1981. Phase Separation of Integral Membrane Proteins in Triton X-114 Solution. J Biol Chem. 1981 Feb 25;256(4):1604-7. PMID: 6257680.

Botchkin L.M. & Matthews, G. 1994. Voltage-dependent sodium channels develop in rat retinal pigment epithelium cells in culture. Proc Natl Acad Sci May 10;91(10):4564-8. doi: 10.1073/pnas.91.10.4564. PMID: 8183948; PMCID: PMC43826.

Bulletin 3133: Molecular Weight Determination by SDS-PAGE. Electrophoresis. Bio-Rad Laboratories, Inc. https://www.bio-rad.com/webroot/web/pdf/lsr/literature/Bulletin_3133.pdf (accessed 11/2020)

Carpenter, E.P., Beis, K., Cameron, A.D. & S. Iwata. 2008. Overcoming the challenges of membrane protein crystallography. Curr. Opin. Struct. Biol. 18:581–586. doi: 10.1016/j.sbi.2008.07.001.

Catterall W.A. 2000. From Ionic Currents to Molecular Review Mechanisms: The Structure and Function of Voltage-Gated Sodium Channels. Neuron; 26(1):13-25. doi: 10.1016/s0896-6273(00)81133-2.

Dunn K.C., Aotaki-Keen, Putkey F.R. & Hjelmeland L.M. 1996. ARPE-19, A Human Retinal Pigment Epithelial Cell Line with Differentiated Properties. Exp Eye Res. Feb;62(2):155-69. doi: 10.1006/exer.1996.0020. PMID: 8698076.

Fine S.L., Berger J.W., Maguire M.G., & Ho, A.C. 2000. Age-related Macular Degeneration. N Engl J Med. 2000 Feb 17;342(7):483-92. doi: 10.1056/NEJM200002173420707. PMID: 10675430.

Fox, J.A. & R.H. Steinberg. 1992. Voltage-dependent currents in isolated cells of the turtle retinal pigment epithelium. J. Physiol. Pflugers Arch. 420, 451–460 (1992). doi: 10.1007/BF00374619.

Fronk, A.H. and E. Vargis. 2016. Methods for culturing retinal pigment epithelial cells: a review of current protocols and future recommendations. J. Tissue Eng. Vol 7: 1–23. doi: 10.1177/2041731416650838

Gräslund, S., Nordlund, P. et al. Structural Genomics Consortium. 2008. Protein production and purification. Nat Methods 5, 135–146. doi: 10.1038/nmeth.f.202

Jager, R.D., Mieler, W.F. & J.W. Miller. 2008. Age-Related Macular Degeneration. N Engl J Med. 12;358(24):2606-17. doi: 10.1056/NEJMra0801537. Erratum in: N Engl J Med. 16;359(16): 1736. PMID: 18550876.

Jha, B.S. & K. Bharti. 2015. Regenerating Retinal Pigment Epithelial Cells to Cure Blindness: A Road Towards Personalized Artificial Tissue. Curr Stem Cell Rep.; 1(2): 79–91. doi:10.1007/s40778-015-0014-4.

Johansson, J.K., Viivi I. Karema-Jokinen, V.I., Hakanen, S., Jylhä A., Uusitalo H., Vihinen-Ranta M., Skottman H., Ihalainen T.O. & Nymark S. 2019. Sodium channels enable fast electrical signaling and regulate phagocytosis in the retinal pigment epithelium. BMC Biol. 2019 Aug 15;17(1):63. doi: 10.1186/s12915-019-0681-1. PMID: 31412898; PMCID: PMC6694495.

Kniesel U. & Wolburg H. 1993. Tight junction complexity in the retinal pigment epithelium of the chicken during development. Neurosci. Lett. 149, 71-74 71. doi:10.1016/0304-3940(93)90350-T.

Kuznetsova A.V., Kurinov A.M. & Aleksandrova M.A. 2014. Cell Models to Study Regulation of Cell Transformation in Pathologies of Retinal Pigment Epithelium. J. Ophthalmol. Article ID 801787. doi: 10.1155/2014/801787.

Kwong K. & Carr M.J. 2015. Voltage-gated sodium channels. Curr Opin Pharmacol, 22:131–139. doi: 10.1016/j.coph.2015.04.007.

LaVail M.M. 1976. Rod Outer Segment Disk Shedding in Rat Retina: Relationship to Cyclic Lighting. Science. 3;194(4269):1071-4. doi: 10.1126/science.982063. PMID: 982063.

Loussouarn G., Sternberg D., Nicole S., Marionneau C., Le Bouffant F., Toumaniantz G., Barc J., Malak O.A., Fressart V., Péréon Y., Baró I. & F. Charpentier. 2016. Physiological and Pathophysiological Insights of NaV1.4 and Nav1.5 Comparison. Front. Pharmacol. 6:314. doi: 10.3389/fphar.2015.00314

MacPhee D.J. 2010. Methodological considerations for improving Western blot analysis. Journal of Pharmacological and Toxicological Methods 61, 171–177. doi: 10.1016/j.vascn.2009.12.001.

Marban E., Yamagishi T. & Tomaselli G.F. 1998. Topical Review. Structure and function of voltage-gated sodium channels. J Physiol. 1;508 (Pt 3):647-57. doi: 10.1111/j.1469-7793.1998.647bp.x. PMID: 9518722; PMCID: PMC2230911.

Matar-Merheb R., Rhimi M., Leydier A., Huche F., Galian C., Desuzinges-Mandon, E., Ficheux D., Flot D., Aghajari N., Kahn R., Di Pietro A., Jault J.M., Coleman A.W. & Falson P. 2011. Structuring Detergents for Extracting and Stabilizing Functional Membrane Proteins. PLoS One. 31;6(3):e18036. doi: 10.1371/journal.pone.0018036. PMID: 21483854; PMCID: PMC3069034.

Mazzoni F., Safa H. & Finnemann S.C. 2014. Understanding photoreceptor outer segment phagocytosis: Use and utility of RPE cells in culture. Exp Eye Res. 126:51-60. doi: 10.1016/j.exer.2014.01.010. Epub 2014 Apr 26. PMID: 24780752; PMCID: PMC4145030.

Modrek B. and Lee C. 2002. A genomic view of alternative splicing. Nat Genet 30, 13–19. https://doi.org/10.1038/ng0102-13

Moody M.F. & Robertson J.D. 1960. The Fine Structure of Some Retinal Photoreceptors. J Biophys Biochem Cytol. 1960 Feb;7(1):87-92. doi: 10.1083/jcb.7.1.87. PMID: 14423794; PMCID: PMC2224851.

NaV1.4: Sodium channel protein type 4 subunit alpha. P35499, SCN4A, *Homo sapiens*. UniProtKB. https://www.uniprot.org/uniprot/P35499 (accessed 11/2020)

NaV1.5: Sodium channel protein type 5 subunit alpha. Q14524, SCN5A, *Homo sapiens*. UniProtKB. https://www.uniprot.org/uniprot/Q14524#similar_proteins (accessed 11/2020)

NaV1.6: Sodium channel protein type 8 subunit alpha. Q9UQD0, SCN8A, *Homo sapiens*. UniProtKB. https://www.uniprot.org/uniprot/Q9UQD0 (accessed 11/2020)

NaV1.8: Sodium channel protein type 10 subunit alpha. Q9Y5Y9, SCN10A, *Homo sapiens*. UniProtKB. https://www.uniprot.org/uniprot/Q9Y5Y9 (accessed 11/2020)

Niegowski D., Hedren M., Nordlund P. & Eshaghi S. 2006. A simple strategy towards membrane protein purification and crystallization. Int. J. Biol. Macromol. vol 39, pp 83–87 doi: 10.1016/j.ijbiomac.2006.02.011.

Ohlendieck K. 1996. Extraction of Membrane Proteins. Methods Mol Biol. 59:293-304. doi: 10.1385/0-89603-336-8:293. PMID: 8798208.

Ohlendieck K. 2004. Removal of Detergent From Protein Fractions. Methods Mol Biol. 244:295-300. doi: 10.1385/1-59259-655-x:295. PMID: 14970566.

Plummer N.W., McBurney M.W., & Meisler M.H. 1997. Alternative Splicing of the Sodium Channel SCN8A Predicts a Truncated Two-domain Protein in Fetal Brain and Non-neuronal Cells. J. Biol. Chem.19;272(38):24008-15. doi: 10.1074/jbc.272.38.24008. PMID: 9295353.

Plummer N.W., Galt J., Jones J.M., Burgess D.L., Sprunger L.K., Kohrman D.C. & Meisler M.H. 1998. Exon Organization, Coding Sequence, Physical Mapping, and Polymorphic Intragenic Markers for the Human Neuronal Sodium Channel Gene SCN8A. Genomics. 1;54(2):287-96. doi: 10.1006/geno.1998.5550. PMID: 9828131.

Reichhart N. & Strauß O. 2014. Ion channels and transporters of the retinal pigment epithelium. Exp. Eye Res. 126; 27e37. http://dx.doi.org/10.1016/j.exer.2014.05.005.

Rigaut G., Shevchenko A., Rutz B., Wilm M., Mann M. & Séraphin B. 1999. A generic protein purification method for protein complex characterization and proteome exploration. Nat Biotechnol. 17(10):1030-2. doi: 10.1038/13732. PMID: 10504710.

Sample preparation for Western blot. Western blot protocols. Abcam plc. https://www.abcam.com/protocols/sample-preparation-for-western-blot (accessed 11/2020)

Santoni V., Molloy M. & Rabilloud T. 2000. Membrane proteins and proteomics: Un amour impossible? Electrophoresis. 21(6):1054-70. doi: 10.1002/(SICI)1522-2683(20000401)21:6<1054:AID-ELPS1054>3.0.CO;2-8. PMID: 10786880.

Schagger H. 2003. SDS Electrophoresis Techniques. Membrane Protein Purification and Crystallization 2/e: A Practical Guide. Doi: 10.1016/B978-012361776-7/50005-X

Schneider C.A., Rasband W.S. & Eliceiri K.W. 2012. NIH image to ImageJ: 25 years of image analysis. Nat Methods. 9:671–5. https://doi.org/10.1038/nmeth.2089

Seddon A.M., Curnow P. & Booth P.J. 2004. Review: Membrane proteins, lipids and detergents: not just a soap opera. Biochim Biophys Acta Biomembr. 1666, 105–117 doi: 10.1016/j.bbamem.2004.04.011

Sparrow J.R., Hicks D., & Hamel C.P. 2010. The Retinal Pigment Epithelium in Health and Disease. Curr Mol Med.; 10(9): 802–823. doi:10.2174/156652410793937813.

Speers A.E. & Wu C.C. 2007. Proteomics of Integral Membrane Proteins Theory and Application. Chem. Rev., Vol. 107, No. 8, 3687−3714. doi: 10.1021/cr068286z. PMID: 17683161.

Strauss O. 2005. The Retinal Pigment Epithelium in Visual Function. Physiol Rev 85: 845–881; doi:10.1152/physrev.00021.2004.

Strunnikova N.V., Maminishkis A., Barb J.J., Wang F., Zhi C., Sergeev Y., Chen W., Edwards A.O., Stambolian D., Abecasis G., Swaroop A., Munson P.J. & Miller S.S. 2010. Transcriptome analysis and molecular signature of human retinal pigment epithelium. Hum Mol Gene, Vol. 19, No. 12 2468–2486. doi:10.1093/hmg/ddq129

Taguchi Y., Mistica A.M.A, Kitamoto T. & Schätzl H.M. 2013. Critical Significance of the Region between Helix 1 and 2 for Efficient Dominant-Negative Inhibition by Conversion-Incompetent Prion Protein. PLoS Pathog 9(6): e1003466. doi: 10.1371/journal.ppat.1003466

Taguchi Y. & Schätzl H.M. 2014. Small-scale Triton X-114 Extraction of Hydrophobic Proteins. *Bio-protocol* 4(11): e1139. doi: 10.21769/BioProtoc.1139.

Vinothkumar K.R. & Henderson R. 2010. Structures of membrane proteins. Q Rev Biophys 43, 1, pp. 65–158. doi:10.1017/S0033583510000041

Von Jagow G., Link T.A. & Schagger H. 2003. Purification Strategies for Membrane Proteins. Membrane Protein Purification and Crystallization 2/e: A Practical Guide. doi: 10.1016/B978-012361776-7/50002-4.

Western blot analysis. Protocols. Alomone Labs. https://www.alomone.com/western-blot-analysis (accessed 11/2020)

Western Blot Troubleshooting. Bio-Rad. https://www.bio-rad-antibodies.com/western-blot-troubleshooting.html (accessed 11/2020)

Wimmers S., Karl M.O. & Strauss O. 2007. Ion channels in the RPE. Prog Retin Eye Res, 26(3):263-301. doi: 10.1016/j.preteyeres.2006.12.002.

Wood J.N. & Baker M. 2001. Voltage-gated sodium channels. Curr Opin Pharmacol. 2001 Feb;1(1):17-21. doi: 10.1016/s1471-4892(01)00007-8. PMID: 11712529.

Wu C.C., MacCoss M.J., Howell K.E., & Yates III J.R. 2003. A method for the comprehensive proteomic analysis of membrane proteins. Nat Biotechnol. 21(5):532-8. doi: 10.1038/nbt819. Epub 2003 Apr 14. PMID: 12692561.

Wu C.C. & Yates III J.R. 2003. Review: The application of mass spectrometry to membrane proteomics. Nat Biotechnol. 21(3):262-7. doi: 10.1038/nbt0303-262. PMID: 12610573.

Yan Z., Zhou Q., Wang L., Wu J., Zhao Y., Huang G., Peng W., Shen H., Lei J., & Yan N. 2017. Structure of the NaV1.4-b1 Complex from Electric Eel. Cell 170, 470–482. doi: 10.1016/j.cell.2017.06.039.

Young R.W. 1967. The Renewal of Photoreceptor Cell Outer Segments. J Cell Biol. 1967;33(1):61-72. doi: 10.1083/jcb.33.1.61

Yu F.H. & Catterall W.A. 2003. Overview of the voltage-gated sodium channel family. J. Med. Chem. 58 (18) 7093–7118. doi: 10.1021/jm501981g.

APPENDICES

Appendix 1: Reagents

In this section are presented all the reagents used in this experiment and their detailed information. In Table 2 are presented the antibodies and in Table 3 the other reagents.

Table 2. Antibodies used in this study. Here are presented the detailed information (manufacturer, source animal and catalogue number) of the antibodies used in this study. The dilution refers to the dilutions used for the confocal imaging whereas "WB" dilutions used in Western blot.

Antibody	Manufacturer	Source	Cat#	Dilution used
Alexa-Fluor 488 anti-guinea pig IgG	Life Technologies	Goat	A11073	1:200
Alexa-Fluor 488 anti-rabbit IgG	Life Technologies	Goat	A21206	1:200
Alexa-Fluor 568 anti-mouse IgG	Life Technologies	Donkey	A10037	1:200
Alexa-Fluor 568 anti-rabbit IgG	Life Technologies	Goat	A11011	1:200
HRP conjugated anti-rabbit IgG	Abcam	Goat	ab6721	1:20 000
HRP conjugated anti-guinea pig IgG	Abcam	Goat	ab6908	1:20 000
$Na_V1.1$	Alomone Labs	Rabbit	ASC-001	1:200
$Na_V1.2$	Abcam	Mouse	ab99044	1:200
$Na_V1.3$	Alomone Labs	Rabbit	ASC-004	1:200
$Na_V1.4$	Alomone Labs	Rabbit	ASC-020	1:200, WB

$Na_V1.4$	Abcam	Rabbit	ab65165	WB 1:5000
$Na_V1.5$	Alomone Labs	Guinea pig	AGP-008	1:200, WB 1:500
$Na_V1.6$	Alomone Labs	Rabbit	ASC-009	1:200, WB 1:1000
$Na_V1.7$	Alomone Labs	Rabbit	ASC-008	1:200
$Na_V1.8$	Alomone Labs	Guinea pig	AGP-029	1:200, WB 1:2000
$Na_V1.9$	Alomone Labs	Guinea pig	AGP-030	1:200
Phalloidin Atto 633	Sigma		68825	1:100
ZO-1	Life Technologies	Mouse	33-9100	1:50
ZO-1	Life Technologies	Rabbit	61-7300	1:50

Table 3. The other reagents used in this study. Here are presented the information about the reagents used in this study excluding the antibodies.

Reagent	**Manufacturer**	**Cat#**
100x Antibiotic-Antimycotic	Gibco by Life Technologies	15240-062
Bovine Serum Albumin (BSA) pH5.2	Sigma® Life Science	A8022-50G
EDTA 100x, 1µl/100µl Halt™	Thermo Scientific	87786
FBS, Fetal Bovine Serum	Gibco by Life Technologies	10270-106
(DMEM/F-12(1:1) (1X) + GlutaMAX™-l, Dulbecco's Modified Eagle medium, F-12	Gibco by Life technologies	31331-028

Nutrient Mixture (HAM), 500 ml		
Matrigel	Corning	734-0268
Methanol	Sigma	32213-2.5L-M
Novex NuPAGE™ 3-8 % Tris-Acetate Gel, 1.0 mm x 10 well	Invitrogen	EA0375BOX
Novex Bolt™ MES SDS Running Buffer, 20x	Invitrogen	B0002
Novex Bolt™, LDS Sample Buffer	Life Technologies	B0007
PageRuler™ Plus Prestained Protein Ladder, 10 to 250 kDa	Thermo Scientific™	26619
1 % penicillin-streptomycin solution (Penicillin 10.000 UI/ml Streptomycin 10.000 UI/m)	Lonza	DE17-602E
10x Dulbecco's Phosphate Buffered Saline without Ca and Mg	Lonza	BE17-515P
ProLong Gold antifade reagent with DAPI	Molecular Probes by Life Technologies	P36935

Protease inhibitor cocktail 100x, 1µl/100µl Halt™	Thermo Scientific	87786
RPEM, RPE optimized Medium, 500 ml	LAgen Laboratories	SKU. No. A3359DJ
Trans-Blot® Turbo™ 5x Transfer BufferBuffer	BioRad	10026938
0.1 %Triton™ X-100	Sigma-Aldrich	X100-100ML
Tween® 20	Sigma	P9416-50ML
WesternBright™ ECL, Western blotting detection kit	Advansta	K-12045-D20

Appendix 2: Immunofluorescence staining protocol

Here is presented the detailed immunofluorescence staining protocol used in this project.

1. The growth medium is removed, and the cells are washed twice with 1x PBS (RT).
2. The PBS is removed, and the cells are fixed with ice cold methanol, for 10 min at RT.
3. The methanol is removed, and samples are washed 3x 5 min with 1x PBS (RT).
4. The cells are permeabilised with 0.1 % Triton X-100 (in 1x PBS). After incubation, the TX100 solution is removed.

5. The background is blocked with at RT for 1h with 3 % BSA in 1x PBS with gentle agitation. After incubation, the BSA solution is removed.

6. The primary antibodies are diluted in 3% BSA (in PBS) and incubated on cells for 1h at RT with gentle agitation.

7. Antibody solutions are removed, and cells are washed 3x 5 min with 1x PBS.
8. The secondary antibodies and Phalloidin are prepared in 3% BSA and are incubated on cells at RT in dark for 1h with gentle agitation.

9. The samples are washed 3x 5 min with 1x PBS in dark with gentle agitation.

10. Finally, the samples are mounted with ProLong Gold with DAPI and left to dry in RT overnight in dark. The dried samples are stored in +4 °C.

Appendix 3: Membrane protein extraction protocol

Here is presented the detailed membrane protein extraction protocol with RIPA buffer. This protocol is based on the Abcam membrane protein extraction protocol.

Reagents:

- Lysis buffer: RIPA i.e. Radioimmunoprecipitation assay buffer (self-prepared)
    - 50 mM Tris-HCl pH 7.4
    - 1 % NP-40
    - 0.5 % Na-deoxycholate
    - 0.1 % SDS
    - 150 mM NaCl
    - 100 mM Na-orthovanadate
- Protease Inhibitor Cocktail + EDTA (commercial, Halt, Thermo Scientific)
    - 100x Protease inhibitors
    - 100x EDTA

- 1x PBS
- Ice

Preparation of lysate from a fresh cell culture

1. The cell culture dish is placed on ice and washed with ice-cold 1x PBS.
2. In a separate microcentrifuge tube lysis buffer, protease inhibitor cocktail and EDTA are combined.
    - Lysis buffer volume: 1 ml per $5x10^6$ cells or 75 cm^2 cell culture flask
    - Protease inhibitor cocktail (100x) and EDTA (100x) volumes: 10 µl / 1 ml of lysis buffer
3. PBS is aspirated and the ice-cold lysis buffer is added on the cells. Lysis buffer is shortly incubated on ice.
4. Adherent cells are scraped off of the dish using a pre-cooled (+4 °C) plastic cell scraper and the cell suspension is then gently transferred into a pre-cooled microcentrifuge tube.
5. The lysate is maintained in constant agitation for 30 min at +4 °C.
6. The cell lysate is then centrifuged at +4 °C, for 20 min at 12,000 rcf.
7. The tubes are gently removed from the centrifuge and placed on ice, the supernatant is aspirated and placed in a fresh tube kept on ice. The pellet is discarded.

Preparation of lysate from cell pellet/ampoule

1. The cells are thawed at RT.
2. The growth media is removed by centrifuging at 300 rcf at RT for 5 min.

3. Supernatant i.e. the growth media is discarded.

4. Optional: Cells are washed with ice cold 1x PBS, centrifuged at 300 rcf at RT for 5 min. After this the PBS is discarded and the pellet is saved.

5. In a separate pre-cooled microcentrifuge tube cold lysis buffer, protease inhibitor cocktail and EDTA are combined. The lysis solution is pipetted on the cell pellet and mixed.

    - Volume of the lysis: $1x10^6$ cells = 80 µl

    - Volume of protein inhibitor cocktail and EDTA: 1 µl/100µl of lysate

6. Cell lysate is maintained in a constant agitation for 30 min at 4°C.

7. Lysate is then centrifuged at 4°C, for 20 min at 12,000 rcf.

8. The tubes are gently removed from the centrifuge and placed on ice, the supernatant is aspirated and placed in a fresh tube kept on ice. The pellet is discarded.

Appendix 4: Western blot protocol

Here is presented the detailed Western blot analysis protocol used in this study. This protocol is based on the instructions of the Alomone Labs.

Reagents

- Membrane proteins extracted from the cells of interest.
- Novex 4x Sample buffer
- 1x Novex Bolt MES SDS Running Buffer (diluted in MilliQ water from 20x)
- PageRuler Plus Prestained Protein Ladder (10-250 kD, Thermo Scientific or Fermenta)
- 1x Bio-Rad Transfer Buffer (diluted in MilliQ water from 5x)

- Blocking buffer: 3 % BSA in 1x PBS + 0.1 % Tween-20
- Washing Buffer: 1x PBS + 0.1 % Tween-20
- Antibodies of interest
- ECL Chemiluminescence detection solution i.e. HRP substrate (Advansta WesternBright)

Equipment

- NuPAGE 3-8 % Tris-Acetate Gels (Invitrogen)
- Heating Block
- Novex Bolt Mini Gel Tank
- Bio-Rad Power Supply (PowerPac basic)
- Bio-Rad Trans Blot Turbo Transfer System
- RTA Transfer Kit (Bio-Rad), which includes
    - 5x Transfer Buffer
    - Nitrocellulose membranes
    - Transfer stacks

Sample Preparation:

1. Sample buffer is added to the membrane protein sample.
    - For 4x Novex SB the suitable ratio is 1:3, i.e. 1 part of the 4x SB + 2 parts of protein sample.
2. Samples are heated in sample buffer at 70 ˚C for 10 min.
3. Next the heated samples are loaded in the wells of the gel.
4. SDS-PAGE is performed according to optimised protocol.

SDS-PAGE:

1. NuPAGE gel is removed from the package. The sticker and the comb are removed carefully.
2. The wells of the gel are rinsed with 1x Running buffer.

3. The gel is place in the Novex Mini Gel Tank with the cassette.
4. Tank is filled with 1x Running buffer.
5. The size ladder and the prepared samples are pipetted into the wells.
6. Lid is placed on the gel tank and power cables are plugged in the power supply.
7. Power is turned on and the run can start.
    - 15 min 100V, 15 min 130 V and 18-20 min 150V
8. Gels are removed from the cassettes and carried out with protein transfer and immunostaining.

Protein Transfer:

1. Nitrocellulose membrane and transfer stacks are soaked in 1x Transfer buffer prior to the assembly of the transfer sandwich.

    - 1x membrane and 2x transfer stacks per 1 medium gel.

2. The transfer sandwich including the SDS gel is assembled on the transfer cassette according to the manufacturer's instructions.

3. The cassette is placed in the Bio-Rad Trans Blot Turbo Transfer System and protein transfer is performed according to the manufacturer's instructions.

    - For High MW Program: 1.3 A, 25 V, 10 min

4. After the protein transfer the nitrocellulose membrane is transferred into the blocking solution and the immunostaining is performed.

Immunoblotting:

1. Nitrocellulose membrane is blocked with blocking solution (3% BSA in PBS + 0.1% Tween-20) for 5h at RT with gentle agitation.

2. Blocking solution is discarded and the nitrocellulose membrane is transferred in the primary antibody solution diluted in blocking solution. Primary antibodies are incubated overnight at 4˚C with gentle agitation.

3. Primary antibody solution is discarded, and membrane is washed with washing buffer (1x PBS + 0.1% Tween-20) 3x 15 min at RT with gentle agitation.

4. Next the membrane is incubated in secondary antibody solution diluted in washing buffer for 1h at RT with gentle agitation.

5. Membrane is washed with washing buffer 3x 15 min at RT.

6. Detection is proceeded using an ECL system. If using a commercial kit, perform according to the manufacturer's instructions.

7. Finally, the nitrocellulose membranes are imaged with a gel imaging tool.

Appendix 5: Original Western blot images

In this section are presented the original and uncropped Western blot images showed in the results section. In Figure 5 is presented the $Na_V1.4$, in Figure 6 $Na_V1.5$, in Figure 7 $Na_V1.6$ and in Figure 8 $Na_V1.8$.

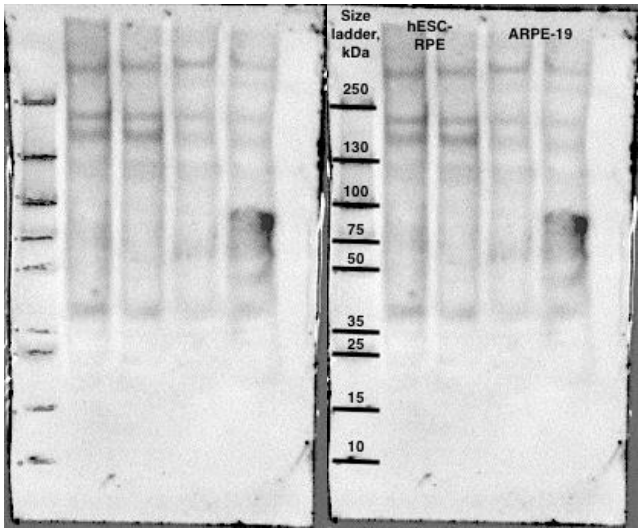

Figure 5. The original image of the $Na_V1.4$ WB results.

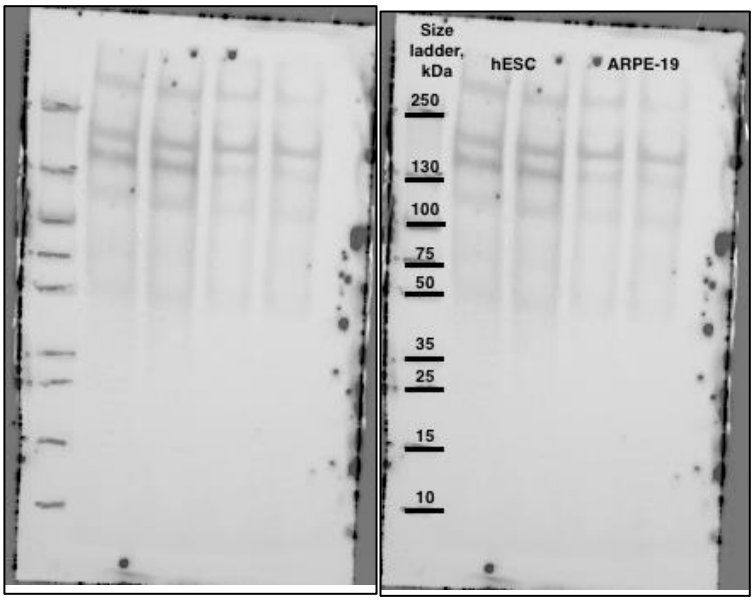

Figure 6. The original image of the Nav1.5 WB results.

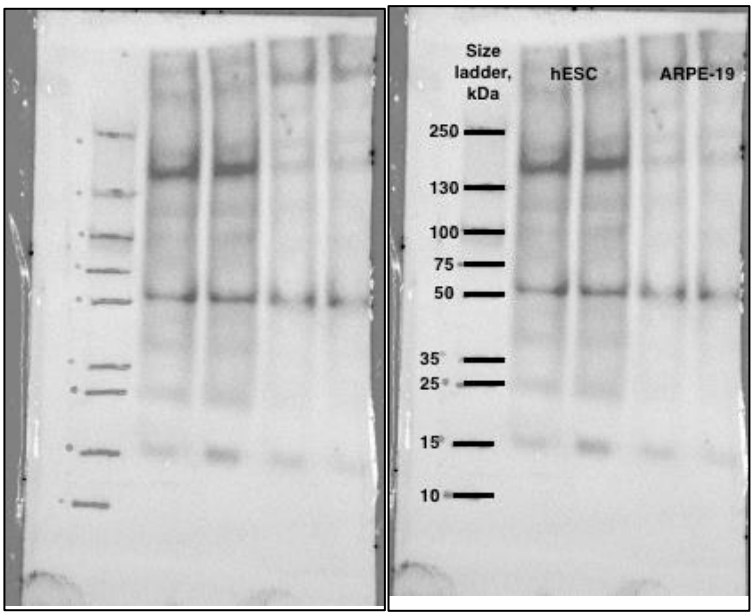

Figure 7. The original image of the Nav1.6 WB results.

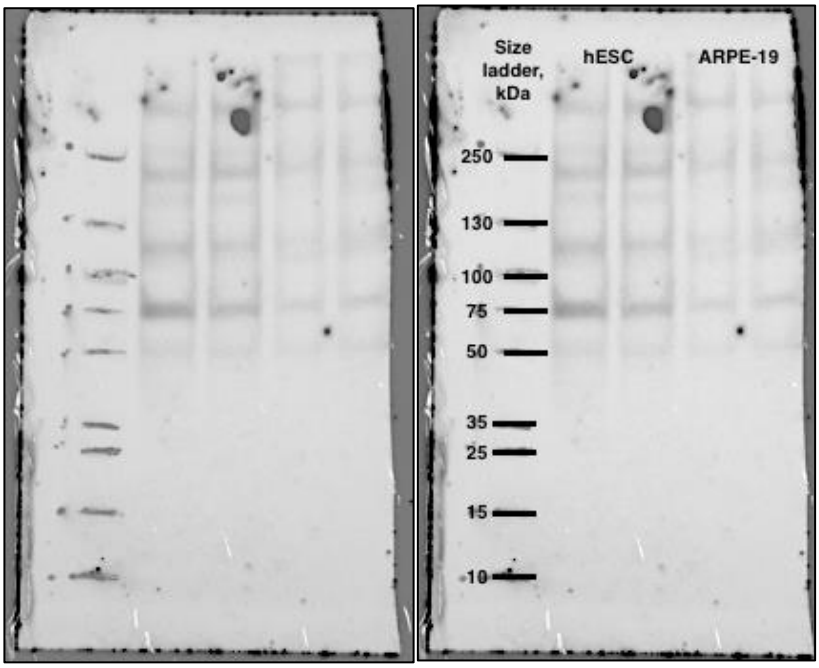

Figure 8. The original image of the $Na_V1.8$ WB results.

Appendix 6: Western blot MW determination

In this section are presented the measurements and calculations of the graphically determined MWs of the WB results. The measurements were defined manually from the images in APPENDIX 5. The measurements of each sample (hESC-RPE or ARPE-19) are means of the two samples in each membrane.

The R_f values were calculated with an equation: $y = mR_f + b \rightarrow MW = 10^y = 10^{mR_f+b}$

$Na_V1.4$

All values for the calculations were defined and measured manually from the Figure 5 (APPENDIX 5). Migration distance of the dye front was 85 mm. The migration measurements, logarithmic size of the standards and the standard R_f values are shown in Table 4. Based on these values the standard curve and curve equation were determined (Figure 9).

Table 4. $Na_V1.4$ measurements for standard curve determinations. Here are shown the logarithmic molecular weight, migration distance and R_f values for each size standard protein. Based on these values the standard curve was formed. The measurements were obtained from Fig. 5.

Size standard (kDa)	**log MW**	**Migration distance (mm)**	**R_f values**
250	2,40	15	0,18
130	2,11	25	0,29
100	2,00	33	0,39
75	1,88	39	0,46
50	1,70	45	0,53
35	1,54	56	0,66
25	1,40	60	0,71
15	1,18	70	0,82
10	1,00	79	0,93

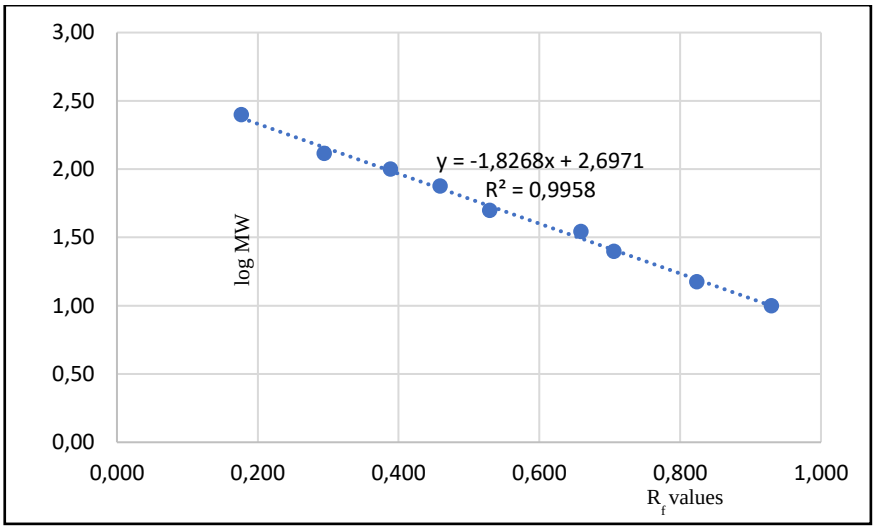

Figure 9. Graphical determination of the $Na_V1.4$ WB standard curve. With this standard curve and a trend line the curve equation could be determined. The x = R_f values of the standard proteins and the y = log MW of the standard proteins. The linear relationship, R^2, shows a strong relationship between standard proteins' MW and migration distance: $R^2 > 0{,}99$. This therefore demonstrates a good reliability for MW predictions.

The equation for $Na_V1.4$ standard curve is $y = -1{,}8268x + 2{,}6971$ (Figure 9), when x = R_f of the unknown protein band. The MW of the bands can then be calculated:

$$\rightarrow y = -1{,}8268x + 2{,}6971 \rightarrow MW = 10^{-1{,}8268R_f + 2{,}6971}$$

The R_f values of the unknown protein bands were inserted in the formula mentioned above. The resulted MWs of each band, and in addition the migration distances and R_f values are presented in Table 5.

Table 5. The unknown protein band information. Here are shown the migration distances, R_f values and molecular weights of the bands visible in the $Na_V1.4$ WB membrane (Fig. 5).

Band of interest	Migration distance (mm)	R_f values	MW (calculated, kDa)
hESC-RPE, 1. band	17	0,200	**215**
hESC-RPE, 2. band	20	0,235	**185**
ARPE-19, 1. band	16	0,188	226
ARPE-19, 2. band	20	0,235	185

$Na_V1.5$

All values for the calculations were defined and measured manually from the Figure 6 (APPENDIX 5). Migration distance of the dye front was 85 mm. The migration measurements, logarithmic size of the standards and the standard R_f values are shown in Table 6. Based on these values the standard curve and equation were determined (Figure 10).

Table 6. $Na_V1.5$ measurements for standard curve determinations. Here are shown the logarithmic molecular weight, migration distance and R_f values for each size standard protein. Based on these values the standard curve was formed. The measurements were obtained from Figure 6.

Size standard MW (kDa)	Size standard log MW	Migration distance (mm)	R_f values
250	2,40	12	0,14
130	2,11	23	0,27
100	2,00	31	0,36
75	1,88	37	0,44
50	1,70	43	0,51
35	1,54	54	0,64
25	1,40	59	0,69
15	1,18	68	0,80
10	1,00	80	0,94

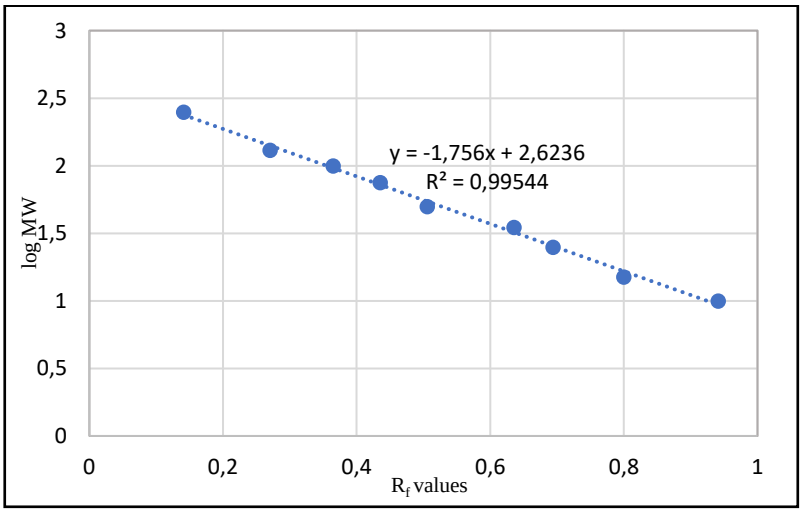

Figure 10. Graphical determination of the $Na_V1.5$ WB standard curve. With this standard curve and a trend line the curve equation could be determined. The x = R_f values of the standard proteins and the y = log MW of the standard proteins. The linear relationship, R^2, shows a strong relationship between standard proteins' MW and migration distance: $R^2 > 0,99$. This therefore demonstrates a good reliability for MW predictions.

The equation for $Na_V1.5$ standard curve is $y = -1{,}756x + 2{,}6236$ (Figure 10), when x = R_f of the unknown protein band. The MW of the bands can then be calculated:

$$\rightarrow y = -1{,}756x + 2{,}6236 \rightarrow MW = 10^{-1{,}756R_f + 2{,}6236}$$

The R_f values of the unknown protein bands were inserted in the formula mentioned above. The resulted MWs of each band, and in addition the migration distances and R_f values are presented in Table 7.

Table 7. The unknown protein band information. Here are shown the migration distances, R_f values and molecular weights of the bands visible in the $Na_V1.5$ WB membrane (Fig. 6).

Band of interest	**Migration distance (mm)**	**R_f values**	**MW (kDa)**
hESC-RPE, 1. band	16	0,19	**196**
hESC-RPE, 2. band	20	0,24	**162**
ARPE-19, 1. band	16	0,19	196
ARPE-19, 2. band	20	0,24	162

$Na_V1.6$

All values for the calculations were defined and measured manually from the Figure 7. Migration distance of the dye front was 85 mm. The migration measurements, logarithmic size of the standards and the standard R_f values are shown in Table 8. Based on these values the standard curve and curve equation were determined (Figure 11).

Table 8. $Na_V1.4$ measurements for standard curve determinations. Here are shown the logarithmic molecular weight, migration distance and R_f values for each size standard protein. Based on these values the standard curve was formed.

Size standard (kDa)	**log MW**	**Migration distance (mm)**	**R_f values**
250	2,40	14	0,16
130	2,11	25	0,29
100	2,00	32	0,38
75	1,88	38	0,45
50	1,70	44	0,52
35	1,54	54	0,64
25	1,40	58	0,68
15	1,18	68	0,80
10	1,00	77	0,91

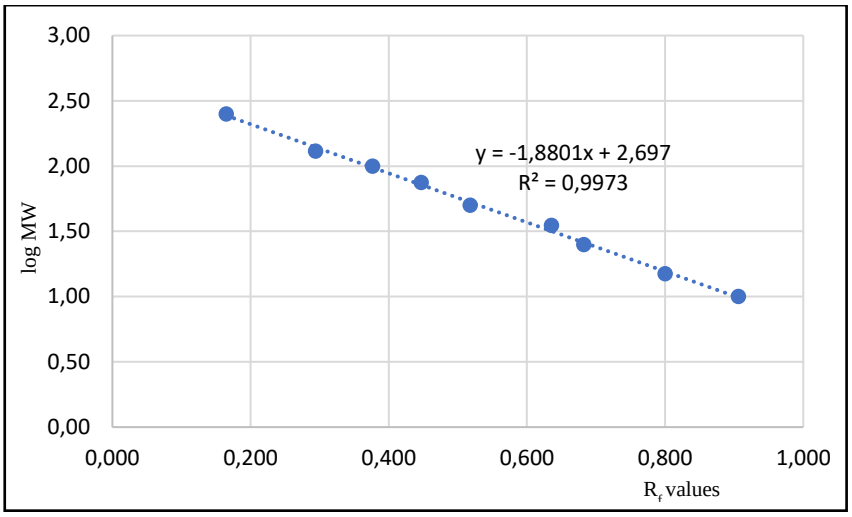

Figure 11. Graphical determination of the Nav1.6 WB standard curve. With this standard curve and a trend line the curve equation could be determined. The x = R_f values of the standard proteins and the y = log MW of the standard proteins. The linear relationship, R^2, shows a strong relationship between standard proteins' MW and migration distance: $R^2 > 0,99$. This therefore demonstrates a good reliability for MW predictions.

The equation for Nav1.4 standard curve is $y = -1,88016x + 2,697$ (Figure 11), when x = R_f of the unknown protein band. The MW of the bands can then be calculated:

$$\rightarrow y = -1,88016x + 2,697 \rightarrow MW = 10^{-1,88016R_f + 2,697}$$

The R_f values of the unknown protein bands were inserted in the formula mentioned above. The resulted MWs of each band, and in addition the migration distances and R_f values are presented in Table 9.

Table 9. The unknown protein band information. Here are shown the migration distances, R_f values and molecular weights of the bands visible in the Nav1.6 WB membrane (Fig. 7).

Band of interest	**Migration distance (mm)**	**R_f values**	**MW (kDa)**
hESC-RPE, 1. band	16	0,19	**220**

hESC-RPE, 2. band	23	0,27	**154**
ARPE-19, 1. band	22	0,26	162
ARPE-19, 2. band	45	0,53	50

$Na_V1.8$

All values for the calculations were defined and measured manually from the Figure 8. Migration distance of the dye front was 85 mm. The migration measurements, logarithmic size of the standards and the standard R_f values are shown in Table 10. Based on these values the standard curve and curve equation were determined (Figure 12).

Table 10. $Na_V1.4$ measurements for standard curve determinations. Here are shown the logarithmic molecular weight, migration distance and R_f values for each size standard protein. Based on these values the standard curve was formed.

Size standard (kDa)	**log MW**	**Migration distance (mm)**	**R_f values**
250	2,40	15	0,18
130	2,11	26	0,31
100	2,00	34	0,40
75	1,88	39	0,46
50	1,70	45	0,53
35	1,54	57	0,67
25	1,40	61	0,72

15	1,18	71	0,84
10	1,00	80	0,94

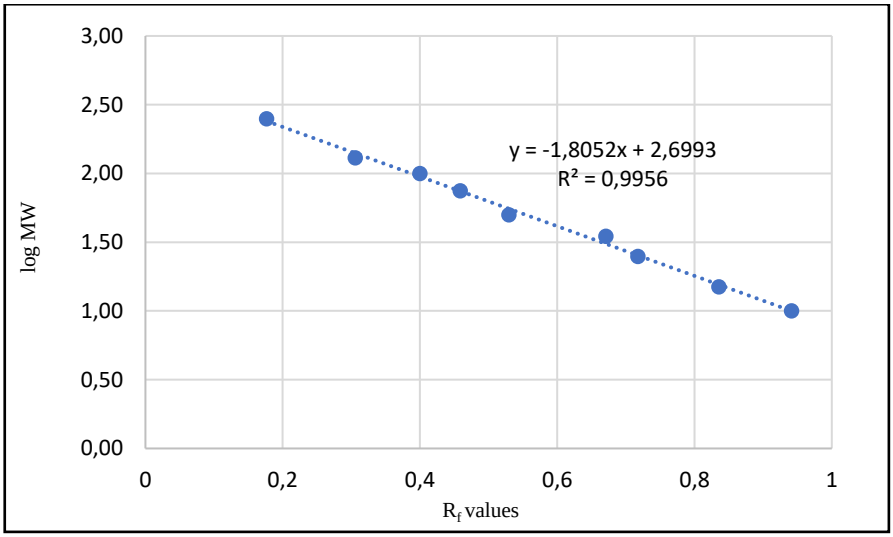

Figure 12. Graphical determination of the Nav1.8 WB standard curve. With this standard curve and a trend line the curve equation could be determined. The x = R_f values of the standard proteins and the y = log MW of the standard proteins. The linear relationship, R^2, shows a strong relationship between standard proteins' MW and migration distance: $R^2 > 0,99$. This therefore demonstrates a good reliability for MW predictions.

The equation for Nav1.4 standard curve is $y = -1,8052x + 2,6993$ (Figure 12), when x = R_f of the unknown protein band. The MW of the bands can then be calculated:

$$\rightarrow y = -1,8052x + 2,6993 \rightarrow MW = 10^{-1,8052R_f + 2,6993}$$

The R_f values of the unknown protein bands were inserted in the formula mentioned above. The resulted MWs of each band, and in addition the migration distances and R_f values are presented in Table 11.

Table 11. The unknown protein band information. Here are shown the migration distances, R_f values and molecular weights of the bands visible in the $Na_V1.8$ WB membrane (Fig. 8). There were multiple faint bands visible in the hESC-RPE lanes, so the MW for each of them was calculated.

Band of interest	**Migration distance (mm)**	**R_f values**	**MW (kDa)**
hESC 1. band	15	0,18	**240**
hESC 2. band	19	0,22	**198**
hESC 3. band	22	0,26	**171**
hESC 4. band	30	0,35	115
hESC 5. band	39	0,46	74
ARPE-19 1. band	17	0,20	218
ARPE-19 2. band	30	0,35	115
ARPE-19 3. band	39	0,46	74